No 727481 RESERVE

D2.7 v1.0

Drafting of Ancillary Services and Network Codes Definitions V2

The research leading to these results has received funding from the European Union's Horizon 2020 Research and Innovation Programme, under Grant Agreement no 727481.

Project Name:	RESERVE
Contractual Delivery Date:	30.09.2019
Actual Delivery Date:	30.09.2019
Contributors:	Álvaro Ortega (UCD), Federico Milano (UCD), Lucian Toma (UPB), Diala Nouti (RWTH), Aysar Musa (RWTH), Catalin Chimirel (Transelectrica), Anca Antemir (Transelectrica)
Workpackage:	WP2 – Frequency Stability by Design
Security:	PU
Nature:	R
Version:	1.0
Total number of pages:	60

Abstract:

This deliverable is an extension of the work presented in D2.6. In this deliverable, recommendations for ancillary services and new network code definitions for frequency control of networks with high penetration of non-synchronous, converter-based generation are drafted. The topics considered for network codes are frequency estimation, RoCoF and fast frequency control with converter interfaced generations and microgrids; and primary and secondary frequency control with renewables and energy storage systems. Both low inertia and 100% non-synchronous scenarios are considered. For the 100% non-synchronous scenario, the concept of linear-swing virtual synchronous generator is discussed. Several case studies duly illustrate the need for new ancillary services and network codes and discuss the performance of the proposed solutions.

Keyword list:

Frequency control, ancillary services, network codes, transmission and distribution networks, frequency estimation, RoCoF, wind energy conversion system, solar photo-voltaic generation, microgrids, energy storage systems, virtual synchronous generator, HVDC systems, transient stability.

Executive Summary

This deliverable, which is the second major output of Task T2.6, discusses, through case studies, the motivations and rationales for the proposal of new ancillary services and network code definitions, or, when possible, the modification of existing ones. The conclusions of this deliverable constitute the final draft of recommendations to be evaluated, harmonized and promoted for international adoption by WP6.

The topics considered include frequency estimation, Rate of Change of Frequency (RoCoF) and fast frequency control with converter-interfaced distributed energy resources and microgrids, and primary and secondary frequency control with renewable energy sources and energy storage systems. Low inertia and 100% non-synchronous scenarios are considered. For the 100% non-synchronous scenario the concept of linear-swing virtual synchronous generator is discussed.

The measure and estimation of the frequency appears as a relevant area of research with also interesting regulatory implications. It is in fact important for transmission and distribution system operators to be able to identify whether distributed resources and/or loads that provide demand response services are regulating the frequency and, if so, the amount of regulation provided. The deliverable discusses a technique to estimate, through a simple yet accurate linear expression, the participation of the aforementioned agents to frequency and RoCoF control based on PMU measurements. This technique is based on the “frequency divider” concept duly discussed in Deliverable D2.1.

Another aspect of the measurement of frequency is the “quality” of the signal to be measured. This appears to be particularly critical in distribution networks. The deliverable discusses a variety of techniques to measure frequency variations aimed at the frequency control through distributed energy resources in distribution networks.

The frequency control of energy storage devices in transmission networks is an effective solution to mitigate the decrease of inertia due to the penetration of renewable non-synchronous generations. On the other hand, energy storage devices are essential in the 100% non-synchronous scenario. The conclusion, based on an exhaustive and comprehensive set of simulation results, is that energy storage devices should be commissioned whenever possible.

The impact of a high penetration of grid-connected microgrids on frequency stability was also studied. The main conclusions are that the microgrids have to provide frequency control and that their energy storage devices are crucial for such a control. The study carried out for this deliverable illustrates a stochastic control technique that, if adopted by all microgrids, is able to maximize their revenues while providing a proper frequency support to the grid. The results identify that the microgrids are incentivized to increase the capacity of their energy storage to increase their revenues and, at the same time, the energy storage allows better tools for regulating the frequency.

With regard to network codes on primary frequency control, it is advisable to develop recommendations for the coordination between inverters considering their characteristics for frequency control and droop values. This is important to achieve coherence in the interconnected power system. Standardized operation characteristics should be provided for those units that respond to both inertial and primary control. This is essential because both control schemes are linked in time, and the power provided as frequency control service is set by the same controller.

With regard to network codes on secondary frequency control, two types of control strategies are considered in this deliverable: the decentralized control specific to the primary frequency control, and the centralized control specific to the secondary frequency control. Both strategies are able to improve the overall dynamic response of the system in the considered scenarios with high penetration of renewable non-synchornous generation. Simulation results suggest that, in the future, a diversity of control procedures may be required.

The 100% non-synchronous scenario is also considered. Assuming that the main converter-based power generation/supply is provided by non-synchronous renewable energy sources and HVDC systems, rethinking the active power control strategy for the electric grid is required. In this deliverable a solution based on the “linear swing dynamics” concepts described in Deliverable D2.3 is discussed and tested through proof-of-concept tests. Results shows that the linear swing dynamics concept is effective and has the potential to maintain the power balance under dynamic conditions in high-voltage transmission systems.

Authors

Partner	Name	e-mail
UCD		
	Álvaro Ortega Manjavacas	alvaro.ortegamanjavacas@ucd.ie
	Federico Milano	federico.milano@ucd.ie
Transelectrica		
	Anca Antemir	anca.antemir@transelectrica.ro
	Catalin Chimirel	catalin.chimirel@transelectrica.ro
UPB		
	Lucian Toma	lucian.toma@upb.ro
RWTH		
	Diala Nouti	dnouti@eonerc.rwth-aachen.de
	Aysar Musa	amusa@eonerc.rwth-aachen.de

Table of Contents

1. Introduction

1.1 Task T2.6

This deliverable is the second major output of Task T2.6 in the Work Package WP2. The main goal of T2.6 is to collect the output of the research performed in WP2 and provide input for the work to be carried out by WP6 with regard to the ancillary services (ASs) and network code (NC) definition concerning frequency control. These inputs from WP2, which take the form of recommendations for the aforementioned services and definitions, will be later evaluated, harmonized and promoted for international adoption by WP6. It is thus crucial for T2.6 to provide a solid foundation of such recommendations, by extending the research carried out in WP2 from the illustrative case studies so far presented, to a broad variety of real-world scenarios.

1.2 Objectives and Outline of the Deliverable

The outputs of T2.6 are collected in two main deliverables, namely D2.6 and D2.7. With regard to this document, D2.7 aims at the following objectives. First, a comprehensive overview of the concept of *electricity market* is provided, which has a crucial importance for the power balancing of the grid, and consequently for the frequency regulation. The evolution of the electricity market in Europe and in the USA is also compared. Second, we discuss the results of the studies carried out on the frequency control strategies that were adequately identified and classified in D2.6. These include: Rate of Change of Frequency (RoCoF) and Primary Frequency Control (PFC) of low-inertia systems; Secondary Frequency Control (SFC) of low-inertia systems; and RoCoF and PFC of zero-inertia systems. Recommendations for updating and/or creating new NC definitions and ASs are also provided and discussed.

1.3 How to Read this Document

This deliverable must be read after all previous deliverables of WP2, namely D2.1 through D2.6. In particular, D2.1, D2.2 and D2.3 are strictly related to Chapters 3, 4 and 5 of this document, respectively; D2.4 and D2.5 give an understanding of all issues related to the telecommunication area that affect, to a greater or lesser extent, all aforementioned chapters; and D2.6 provides the first draft of the recommendations that have been expanded and consolidated in this document. Additional dependencies and links of D2.7 with other deliverables, tasks and work packages from the RESERVE project are summarized below (see Figure 1.1).

- The case studies proposed have been defined based on the different Scenarios on the Frequency defined in D1.1 (T1.1, WP1).
- The research concepts presented in this deliverable and which have been studied during the last year of the project have been tested and validated by T5.3 (WP5) in D5.4 and D5.5.
- We recommend the interested reader to read D3.9 from Task T3.7 of WP3 in parallel to D2.7. The rationale is that T3.7 is responsible of defining the recommendations of ASs and NC definitions concerning voltage control, mirroring the objectives of T2.6 for frequency control concepts. Therefore, the structures of D2.7 and D3.9 are analogous.

1.4 Structure of the Deliverable

This deliverable is the result of the collection of contributions from the different partners that participate in WP2. This deliverable has thus been organized to maximize the coherency of the subtasks performed by each partner, while optimizing the flow of the overall content. To this aim, each chapter spanning from 2 through 5 has been authored by a different institution, as indicated below.

- Chapter 2: Transelectrica;
- Chapter 3: UCD;
- Chapter 4: UPB; and
- Chapter 5: RWTH.

The remainder of this document is organized as follows. Chapter 2 provides an overview of the concept of electricity market, as well as its evolution in Europe and in the USA. The recommendations for updates of existing NCs and ASs based on the results of the studies of the different concepts identified in D2.6 are provided in Chapters 3 through 5. In particular, Chapters 3 and 4 focus on the RoCoF, PFC and SFC of low-inertia systems, whereas Chapter 5 tackles the issues related to zero-inertia systems. Chapter 6 draws concluding remarks and outlines the future work directions beyond the completion of T2.6.

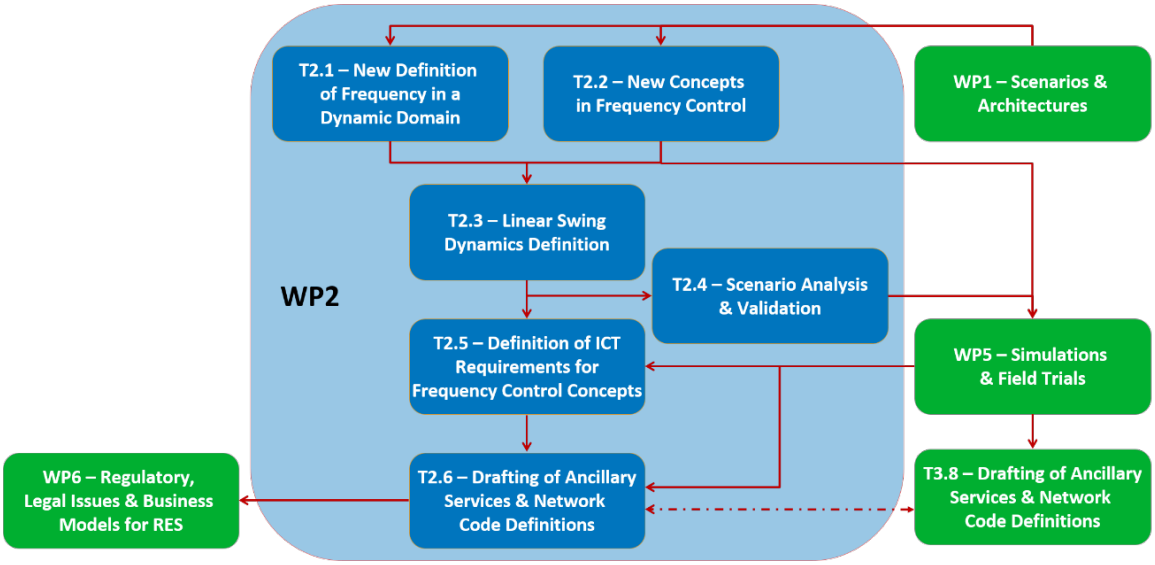

Figure 1.1: Relations between Tasks in WP2 and other Work Packages.

2. Electricity Market

In deliverable D2.6, we provided a detailed review of the existing Network Codes (NCs) defined by the European Network of Transmission System Operators for Electricity (ENTSO-E) that cover frequency regulation. We also outlined a selection of white papers that recommend updating the existing NCs, and that are currently under review by different Transmission and Independent System Operators (TSOs and ISOs) such as Transelectrica from Romania.

In this chapter, we focus on the concept of *electricity market*, which has a remarkable relevance in the medium and long term power balancing, and is a key aspect in the regulation of the frequency.[1]

In particular, this chapter briefly discusses the evolution of the electricity market in Europe.[2] This evolution will also be compared with the situation in the USA.

2.1 Europe

Based on current policy targets and expectations, electricity has a key role in the European Union's (EU's) economy. There are ambitious goals like decarbonization and energy efficiency activities which are expected to decrease the greenhouse gas emissions by 40% in 2030 and 95% in 2050 down to below 1990 levels, increasing the renewable energy share to at least 27% of final energy consumption in 2030, and targeting 27% energy savings by 2030 as compared to business-as-usual rates of growth. Correlated, the electrification and digitalization trends suggest that the share of electrical energy in final energy consumption would grow from above 30% in 2030 to nearly 40% in 2050. Decentralized generation assets, mostly focused on power electronics, would account for more than 30% of all generation capacity in 2030 and could easily exceed half of installed generation capacity by 2050.

There are three subsequent EU Energy Packages, introduced in 1996, 2003, and 2009, dedicated to create a single integrated and competitive European market.

Today, electricity can be traded in the EU via long-term bilateral contracts (representing two-thirds of the electricity transactions concluded in the major markets in 2015) or via the four components of the wholesale power exchanges, namely:

- the forward and derivatives markets (weeks to years in advance);
- the day-ahead markets (DAMs);
- the intraday markets (IMs) (operating for an hour or fractions of an hour); and
- the balancing markets (operating in real time).

By 2015, the yearly trading volumes already reached a few hundred terawatt-hours (TWh) in some European spot markets e.g., the Italian power market exchange (IPEX), the Centre-North European power market exchange (EPEX), and the Scandinavian Nord Pool.

In Europe, the price for the customers contains the sum of the following three main components (see Figure 2.1 for an overall picture of average prices during the third quarter of 2018 in Europe):

- the energy and supply component;
- the network component (tariffs for transmission and distribution); and
- the component comprising taxes, levies, fees, and charges.

There is a large interest for widespread implementation of market coupling-solutions for cross-border congestion management in Europe as a clear example of regional coordination that would contribute to the realization of the internal electricity market. At the time of writing this report, 22 European countries (including the United Kingdom) are coupled in different combinations for the DAM with the goal of improving market liquidity, investment allocation management, and price signals.

[1] The interested reader can refer to Chapter 4 of deliverable D2.1, and Chapter 2 of D2.2 for more details about the relation between power balancing and frequency regulation.

[2] For economy of words, we will henceforth refer to *electricity market* as *market*.

Figure 2.1: Wholesale baseload electricity prices – Third quarter of 2018 [28].

Coupled markets are using a common algorithm for settling market transactions, considering also the constraints of the interconnectors between the countries. We can conclude that the coordination of national energy systems across the EU is beneficial from the standpoints of coordinating generation capacity investment and coupling energy markets. European National Regulatory Authorities approved the proposal under the Commission's Capacity Allocation and Congestion Management (CACM) regulation, (EU) 2015/1222, as introduced by the 17 Nominated Electricity Market Operators (NEMOs) committee defined there. The agreement seeks to establish an European market coupling operator to further integrate DAM and IM functions across Europe. The goals are to increase liquidity by organizing trading between zones and establishing clear and detailed rules harmonized within the NEMOs.

Looking for the safety part of the market, the Balancing market consists usually of ex-ante Ancillary Services Market (ASM) – balancing capacities market – and almost on-line balancing energy markets. The TSOs can take into consideration the valid bids/asks that the participants have issued in the previous ex-ante ASM session. In the balancing energy market, the TSOs will accept energy demand bids and supply offers and they will mobilize as necessary the resources, to provide secondary control services and balance energy injections with withdrawals into/from the grid, in real time. It is now a dedicated approach to involve the citizens more and more in such balancing by aggregated demand request services.

There is a clearly defined schedule to also connect the Balancing Markets within Europe, at least at regional level for all main 4 products:

- Frequency Containment Reserve (FCR);
- automatic Frequency Restoration Reserve (aFRR);
- manual Frequency Restoration Reserve (mFRR); and
- Replacement Reserves (RR).

The transition towards a single, integrated European market (IEM) will surely help as well by allowing more and more cross-border exchanges of balancing services. To guarantee nondiscrimination, all of these mechanisms are designed in such way that, regardless of the country in which a generator is located, it could bring its contribution to regional or continental power system stability.

EU has decided for a “regional” approach to European energy policies, thus most of the electricity system and market aspects are addressed via aggregations of neighboring countries within such regions.

There is a clear target to have transparency of market results after the operation day. Therefore, there is already a transparency platform managed by ENTSO-E where results are filled in by each market operator and TSO after the operation day.

A suitable and appropriate market design will most likely be the most important factor for achieving the single European Power Market in the near future. It is important to note that CACM regulation represents a key moment for Europe’s integration of electricity markets. On the other hand, the capacity calculation and allocation principles described there represent only the first step and still all other issues like time frame, standard products and many others will need to be addressed in line with “COMMISSION REGULATION (EU) 2017/2195 of 23 November 2017 establishing a guideline on electricity balancing” provisions.

2.2 United States of America

After issuing the order 888 from the Federal Energy Regulatory Commission (FERC) in 1996, the USA power industry began its restructuring process. This undertaking generally involved a clear transition from vertically integrated utility structures, where generation, transmission, and distribution are combined to serve consumers, to the unbundling systems. Through moving to a market environment, generation companies (GenCos) can now compete with each other to provide energy through open access transmission and distribution systems managed by transmission (TransCos) and distribution companies (DisCos). The goals of the restructuring are the efficient production of electricity and efficient generation investment through competition.

Wholesale electricity markets are managed by independent system operators (ISOs) or regional transmission organizations (RTOs), whose responsibility is a reliable system operation, market administration, and system planning. GenCos, large consumers, load aggregators, marketers, and load serving entities (LSEs) buy and sell electricity through FERC regulated wholesale electricity markets.

USA electricity markets have been considered largely successful, and the RTO footprint continues to grow. Today there are seven RTOs within States.

Wholesale electricity markets evolved with changes in regulatory policy, technological innovations, and economic conditions since the start of electric restructuring. During the past two decades, the USA power industry has experienced a transformation with the retirement of coal, oil, and nuclear resources; increased electricity production and investment in natural gas facilities due to environmental and siting factors as well as relatively low gas prices; increased penetration of renewable resources as a result of state environmental policies; and an increase in demand resources and distributed generation technologies. These changes have created challenges to power system operation and planning and electricity market design.

Wholesale electricity markets emerged in the USA in the late 1990s with different models. PJM Inter-

connection and New York ISO (NYISO) started locational marginal pricing (LMP)-based energy markets with a two-settlement system in 1998 and 1999, respectively. California ISO (CAISO) adopted a day-ahead power exchange with the real-time energy market in 1998. ISO-NE opened its real-time energy market with a single market clearing price and an uplift payment-based congestion management model in 1999. After the California energy crisis in the early 2000s, the power exchange model was considered to facilitate market power abuse and gradually abandoned in the USA.

Today model involves a set of common features, including the two-settlement system (DAM and real-time market (RTM)), LMP, co-optimization of energy and ASs, zonal reserve products, financial transmission rights, and a forward capacity market.

Energy is the main product traded in USA electricity markets, which typically include the DAM and the RTM. Although market designs vary in different ISO regions, all have structured the two markets in a two-settlement system with the forward DAM and the spot RTM. All markets also have a similar objective of maximizing the total social surplus, and LMP is used to manage the transmission congestion.

Energy trading in the ISO managed wholesale markets often creates two financial positions for each market participant: DAM and RTM (cleared transaction quantity). A two-settlement system is adopted to settle each financial position.

In addition to meeting the system load, power system operators have to prepare for generation contingencies and load fluctuations in real time. These additional reliability needs can be satisfied by AS products besides energy (as examples: regulation, reserves, and ramping). Resources with these additional capabilities are compensated through the ASM. AS products could be quite different among ISOs because the ISO systems may have different reliability needs. Consequently, the ASMs are diverse. CAISO considers a 5-min ramping product, Mid-continent ISO projects a 10-min ramping product, and ISO-NE does not currently have a ramping product. With the increasing penetration of renewables, new system features arise and may create a need for new ASs.

Because energy and ASs share the capacity of generation units and transmission network, they are often co-optimized to achieve the most efficient capacity allocation of resources, leading to a scheduling optimization problem that simultaneously determines the energy and ASs designations for resources.

Currently, the power industry is facing yet another revolutionary change. Government directives to lower the carbon footprint and, as a consequence, high penetration of renewable energy resources and smart grid technologies are transforming power system planning and operational paradigms. Distributed energy resources (DERs) are being built deeply into the distribution networks, and the boundary between transmission and distribution is blurring. A significant part of DERs is unobservable to the transmission system operators, introducing an unprecedented level of uncertainty not only spatially but also temporally due to the intermittent nature of renewable resources.

The unprecedented level of uncertainty due to the high penetration of renewable resources and DERs requires more flexibility to deal with uncertainty. This leads to the need for a new flexibility market mechanism to create incentives for investment in flexible technologies. Some ISOs, such as CAISO, have introduced a 5-min ramping product to accommodate the step change of the load curve due to significant swings in photovoltaic production. The design of such a new product should consider its interaction with existing products, such as reserves. It is important that the new products provide unique and different services from the existing products so as to attract targeted flexible resources.

2.3 Romania

This Section provides updated values of the tables and graphs discussed in Section 2.2 of D2.6 which break down the total power generation in the Romanian power system according to the generation technology. Values are from 1 April 2019, and are listed in the remainder of this Section.

Table 2.1: Installed capacities in the Romanian transmission system on 1 April 2019.

Technology	Dispatching units [MW]	Non-dispatching units [MW]	Total [MW]
Coal	5,915.00	317.20	6,232.20
Oil and gas	4,335.60	1,120.47	5,456.07
Hydro	6,163.33	595.45	6,758.78
Wind	2,955.80	75.77	3,031.57
Biomas/biogas	29.65	102.33	131.98
Photovoltaic	604.12	778.24	1,382.36
Nuclear	1,413.00	0.00	1,413.00
Geothermal	0.00	0.05	0.05
Total	**21,416.50**	**2,989.51**	**24,406.01**

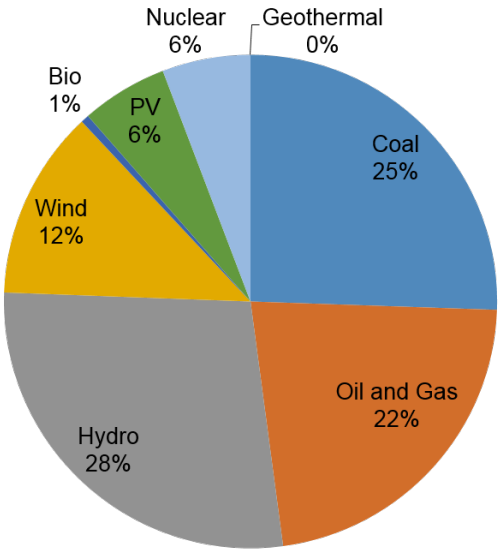

Figure 2.2: Shares of installed capacity in the Romanian transmission system on 1 April 2019.

Table 2.2: Breakdown of maximum instantaneous consumption and generation on 1 April 2019.

Consumption [MW]	**9,541**
Production [MW]	**10,484**
Coal	2,482
Oil and gas	2,184
Hydro	1,934
Wind	13
Biomas/biogas	66
Photovoltaic	-1
Geothermal	0
Nuclear	1,345
Import	**1,601**

3. Drafting of Ancillary Services and Network Code Definitions for Frequency Estimation and for the Provision of RoCoF and Fast Frequency Control

This chapter considers the ASs and NCs described in Chapter 2 of D2.6 that are related to the RoCoF and fast PFC in low-inertia systems. In particular, the chapter focuses on the codes that need to be updated and, more often than not, created in order to account for the new agents that are expected to participate, to a large extent, to these frequency control categories in the near future. Examples of these agents are DERs operated by Distribution System Operators (DSOs) (Section 3.1), non-synchronous frequency makers (Section 3.2), Converter-Interfaced Energy Storage Systems (CI-ESSs) (Section 3.3), and grid-connected microgrids (Section 3.4).

3.1 Frequency Control of Distributed Energy Resources in Distribution Networks

As discussed in Section 3.1.2 of Deliverable D2.6, until recent years, frequency regulation from DERs was not available, as they were operated with the aim of supplying their maximum feasible power according to meteorological conditions by means of the maximum power point tracking (MPPT) control [48, 50]. However, this scenario is rapidly changing. In fact, as the penetration of DERs increases, there is the urgent need to maintain the system frequency regulation capability while the system inertia is being reduced. A crucial problem is that, while active power curtailment is generally always available for DERs in case of over-frequencies, they usually cannot guarantee a power reserve in case of under-frequencies. To overcome this issue, CI-ESSs become apparent, thanks to their capability to supply/absorb large amounts of active and reactive power simultaneously in very short time frames [43].

This Section discusses the results of the comprehensive analysis on the impact of the frequency control of distribution-level DERs on the overall transient behavior of transmission systems that has been carried out in this project. Three strategies to generate the signal used as input of the DER frequency regulators have been proposed and compared: (i) decentralized, where each DER estimates its local frequency through a Phase-Locked Loop (PLL); (ii) centralized, where the DERs connected to the same distribution system receive a common signal from a PLL installed at the point of contact of the distribution network with the transmission system; and (iii) average, where the frequency estimations of the DERs are collected at the distribution system level and then a common, average signal is sent back to each DER. For each strategy, different configurations of the techniques and devices used to generate the frequency signal have been compared. The case study also duly discusses the effect of noise, delay in the transmission of the signals and loss of information in the communication system. The bulk of references [41, 42, 43, 44] collects the formulation of each of the concepts studied, and the results obtained.

Results of this study have been gathered and discussed in D2.5, where requirements for the ICT used to transmit the different signals have been defined from this work, and in the remainder of this Section, which provides the recommendations of ASs and NC definitions for DERs connected at the distribution system level and providing frequency regulation.

Based on all simulation results, the following remarks and recommendations are relevant.

- The accuracy and the sensitivity to noises present in the input signal of five PLL configurations used for frequency estimation, namely (i) the synchronous reference frame (SRF)-PLL, (ii) the low-pass filter (LPF)-PLL, (iii) the Lag-PLL, (iv) the enhanced E-PLL, and (v) the second-order generalized integrator (SOGI)-FLL. Analysis of simulation results allows the conclusion to be drawn that the LPF-PLL has the best performance overall, as it provides the most accurate frequency estimation after fast and large frequency variations caused by contingencies such as faults and line outages, and it also shows the least sensitivity to noise present in the bus voltage angles. Good overall performance is also achieved by the commonly-used SRF-PLL and the Lag-PLL. Finally, the worst accuracy, and the

highest sensitivity to noise are observed from the E-PLL, and to a greater extent, from the SOGI-FLL.

- The local fast frequency control provided by converter-interfaced DERs shows a good overall performance when using the SRF-PLL and the LPF-PLL compared to the scenario where the *ideal* signal obtained with the Frequency Divider Formula (FDF) [34], proposed in D2.1. Noise and numerical spikes do not appear to significantly deteriorate the quality of the control, provided that such DERs include a proper low-pass filter within their primary frequency controllers. On the other hand, filtering should not introduce a delay in the frequency measure to prevent the deterioration in the dynamic response.
- Fast dynamics such as those of fluxes can deteriorate the dynamic response of PLL-based frequency controllers. Simulation results show that, in some cases, the numerical derivative of the bus voltage phase angle of the PLL can lead to non-physical oscillations and, possibly to numerical instabilities.
- The average rotor speed provided by the center of inertia (CoI), which is commonly used in practice, intrinsically filters local frequency variations. This fact may cause poorly-damped frequency oscillations, especially if coupled to devices with a slow response, such as thermostatically-controlled loads.
- The centralized strategy to retrieve the input signal of the frequency controllers of the DERs located in a given distribution network shows a better overall performance compared to the decentralized and the average (distributed) approaches. However, the performance of the centralized strategy highly depends on the associated signal communication delays. Since the centralized approach depends on a single Phasor Measurement Unit (PMU) connected at the point of common coupling with the transmission grid, in order to avoid the loss of all regulation capability in case of malfunctions of the measurement device, a redundancy of such a measure is desirable.
- The decentralized strategy works reasonably well, and it does not include any form of communication delay. However, its overall performance can be highly deteriorated in case of loss of any of the frequency measures.
- The average strategy shows a good robustness against the loss of measurement signals without the need of redundant measures. It naturally filters out the largest spikes and other numerical issues of the measures during transients. Similarly to the centralized strategy, its performance highly depends on the communication delays.

3.2 Frequency Estimation: Frequency Takers and Frequency Makers

In deliverables D2.1, D2.2 and D2.3 we have comprehensively discussed the potential of non-synchronous generation to provide frequency control [32]. These studies consider several technologies, including wind generation [4, 23, 36], solar PV generation [1, 11, 26], VSC-HVDC links [24], energy storage devices [40, 45, 49], and thermal loads [2, 5, 52].

As introduced in Chapter 3 of D2.6, a current challenge for the secure operation of the grid is the ability of TSOs to determine through simple measurements whether non-conventional devices provide frequency control at a given time. Some TSOs have *resolved* the problem by measuring the active power output and “trusting” the non-conventional devices, which clearly exposes the system to potential security issues if the control is not provided or not available when needed. Other TSOs prefer to allocate conventional frequency reserve, which guarantees a secure operation but leads to higher energy costs.

This is thus a major concern for system operators and prevents relying on and properly rewarding the devices that provide such frequency support. Smart metering is already a reality but it is mostly utilized on the device side to implement the frequency control itself, e.g. [48], rather than on the system operator side.

The need for metrics to define the frequency response and control in a transmission system has been recognized since a decade ago. The report [12], for example, defines three obvious metrics, namely frequency nadir, nadir-based frequency response, and primary frequency response. These are, however, “global” metrics and are adequate only for off-line adequacy and reliability studies. Existing techniques to evaluate the primary frequency and inertial responses are qualitative and based on statistical analysis of time series [7, 8] or on Kalman filtering [3].

The technique proposed in this project is based exclusively on PMUs frequency measurements as well as power measurements at network buses [30, 39]. The technique consists in a further elaboration on the FDF, which has already been utilized to estimate bus frequencies [55], machine rotor speeds [33] and the frequency of the CoI [29]. The proposed approach is conceptually different from existing approaches as it is local, quantitative and aimed at on-line applications. It allows determining, at least in transient conditions and under certain hypotheses, whether a device provides inertial response and/or frequency control (*frequency maker*) or not (*frequency taker*).[1]

A summary of the taxonomy of frequency taker and frequency maker devices is provided in Appendix A. The accuracy, robustness and applicability of the proposed technique have been validated by means of a comprehensive case study based on the dynamic model of the All-Island Irish Transmission System (AIITS) [9, 10]. The size of this system (1,479 buses) and the high penetration of converter-interfaced generation make this system an excellent test-bed to study the features of the proposed evaluation technique that is based on the concept of Rate of Change of Power (RoCoP).

A selection of simulation results are presented in Chapter 5 of Deliverable D5.7. Further results and discussions can be found in [30, 39]. Based on all simulation results, the following remarks and recommendations are relevant.

- In steady state, the index RoCoP goes to zero, which also indicates that, in stationary conditions, all machines rotate at the same speed. Note that it is immaterial the value of such a stationary speed, e.g., if it is different from the synchronous reference if no Automatic Generation Control (AGC) is installed. This result is expected as, in steady state, all frequency controllers are inactive. This result is also consistent with the transient nature of the RoCoP.
- The proposed RoCoP can be used to estimate, in the first seconds after the contingency, the synchronous machine inertias with high accuracy. After these seconds, the trajectories start drifting away from their respective actual values due to the overlapping of the inertial response of the machines with the PFC.
- The RoCoP index can be applied to evaluate the nature of any device, whether it is synchronous or not. These include converter-interfaced generation (wind, solar, etc), energy storage systems, flexible loads, etc.
- The threshold ϵ needs to be defined based on the knowledge of the system under study, and using for example statistical moments such as the standard deviation of the RoCoP of a device or subsystem connected to a particular bus over an extended time window. Note that, as thoroughly discussed in [30, 39], one does not need to know the specific nature of the device/subsystem to define its ϵ, as the RoCoP index is calculated exclusively with network measurements.
- The results indicate that measuring the active power injection is, in general, not a sufficient criterion to remunerate the owners of ancillary service providers for the provision of fast frequency control. With this regard, the RoCoP index appears as a sensible tool for system operators.
- Different thresholds ϵ can be defined for different purposes. For instance, the system operator can define a ϵ_o, common to all devices, above which specific devices or systems are

[1] We prefer the notation *frequency maker* and *frequency taker* versus the notation *grid forming* and *grid following*, as the latter refers exclusively to the control setup of power electronics converters. The concepts discussed in this document are more general and do not refer to a specific device technology.

required to provide fast frequency control. Then, individual, possibly multiple thresholds ϵ_i can be defined for each device or system coupled to fast frequency control to quantify the *amount of control* that has been provided during a specific event.

- The effectiveness of the fast frequency control provided by a device or subsystem does not only depend on its power capacity. The RoCoP can thus be a valuable tool for system operators as it allows to take into account topological, geographical and technical aspects as discussed in the case study discussed in Chapter 5 of D5.7.
- Issues associated to the deterioration of the proposed RoCoP index due to the presence of noise in the measurements can be prevented if the RoCoP is passed through a low-pass filter. The features of the resulting filtered index are fairly similar to those when noise is not considered and thus the filter is not required.

3.3 Frequency Control of Converter-Interfaced Energy Storage Systems in Transmission Grids

There is no doubt that industry is currently betting on energy storage technologies, particularly converter-interfaced ones. This is justified by market predictions. The annual revenue for all storage applications is expected to increase from $220 million in 2014 to $18 billion in 2023. The total power capacity of battery storage will rise from 360 MW to 14 GW over the same period [25].

However, regulatory authorities do not move forward at the same pace as the research and development of these CI-ESSs. In previous deliverables of WP2, we have extensively justified the need for a specific NC for CI-ESSs, which is currently non-existent. Among the number of ASs that CI-ESS can provide, there are: flattening the power provided by Renewable Energy Sources (RESs), active power regulation in a transmission line, local and/or global frequency regulation, RoCoF mitigation, improvement of critical clearing times, local voltage regulation, daily load leveling, etc.

This Section collects a detailed set of recommendations for CI-ESSs for the ASs listed above. Such recommendations are based on a comprehensive set of case studies, which include well-known benchmark networks (WSCC 9-bus, 3-machine system; IEEE 14-bus system; and New-England 39-bus, 10-machine system), as well as a dynamic model of the real-world, 1,479-bus AIITS. All simulation results are collected in the monograph [31], written by the first two authors of this deliverable, and a relevant selection of such results can be found in Deliverables D2.1, D2.6 and D5.7.

A large variety of CI-ESS technologies have been modeled, implemented and simulated. These include battery energy storage (BES), flywheels (FES), superconducting magnetic energy storage (SMES), supercapacitors (SCES), and compressed air storage (CAES), among others. For the sake of the discussion below, two main groups of technologies can be defined, as follows.

- **Fast CI-ESSs**. These CI-ESSs are typically characterized by fast response times (in the order of a few tens of milliseconds) and high number of cycles in their lifetime (up to 100,000), but relatively short discharge times (up to few minutes).[2] Examples of technologies that fall into this category are FES, SMES and SCES.
- **Slow CI-ESSs**. Intuitively, slow CI-ESSs are the opposite of fast CI-ESSs, thus characterized by relatively slow response times (up to several seconds), small number of cycles (up to a few thousand) and long discharge times (up to several hours).

Based on all simulation results, the following remarks and recommendations are relevant. Note that, with the aim of clarity and completeness, we have included below remarks that refer not only to RoCoF and fast frequency control from CI-ESS, but also to conventional primary and secondary frequency control, transient stability and, marginally, to voltage and reactive power supports.

[2] The *response time* is the time required by the CI-ESS to charge or discharge at rated power from standby. The *discharge time* is the time required to discharge, at the rated power, a fully charged storage device.

1. **RoCoF and Fast Primary Frequency Control**
    - It is recommended to install hybrid ESSs (HESSs) composed of one fast (e.g., a FES) and one slow (e.g., a BES) ESS technology. With this configuration, the system can benefit from the fast response of the FES for filtering fast transients ($\leq$ 1 minute), while the BES provides active power reserves over longer periods thanks to its higher energy capacity and power rate.
    - Key aspects such as the CI-ESS location and the tuning of the control parameters are crucial from the control performance and stability points of view. In this regard, decisions must be made based on a deep knowledge of the power system under study (e.g., its topology).
    - The installation of a single HESS in the AIITS helped reduce the power oscillations in a transmission line due to a large contingency (short-circuit) by about 60%. The same HESS reduced by over 30% the frequency nadir at the bus where it is connected after the loss of one synchronous generator with respect to the case without HESS.
    - An aspect that needs to be carefully considered is the reach of current limits of the power converter and/or energy limits of the CI-ESS during a contingency. Such saturations cause transients in the system that can be even worse than the initial contingency and, in the long term, can deteriorate the components of the converter and shorten the operational life of the overall storage device.
    - Current limits of the HESS are overall more likely for higher penetrations of RESs. As this share increases, the total inertia of the system is reduced, making the system less resilient to large perturbations, which in turn results in higher variations of active power flows in transmission lines and bus frequencies, and thus, to a greater contribution of the HESS.
    - Two solutions are proposed to help prevent current saturations: (i) increasing the installed capacity of HESSs proportionally to the penetration of RESs, and (ii) the design of more sophisticated control strategies for CI-ESSs. Simulation results prove that more advanced strategies than the conventional Proportional-Integral Control (PIC), such as Sliding Mode Control (SMC) and H-infinity Control (HIC), contribute to a more efficient use of the storage device, thus statistically reducing the saturations of the power converter, at least of the slow CI-ESSs.
    - HIC and SMC also outperformed the PIC on the reduction of the frequency nadir after a contingency. Nevertheless, PIC shows a fair robustness against a wide range of loading conditions and contingencies, and system uncertainties.
    - For RoCoF mitigation, within WP2 it has been proposed a solution that allows for a full control capability of the storage device for the time frames of both inertial response (up to 4-5 seconds) and primary frequency control (up to tens of seconds). This approach combines a droop and a RoCoF regulation channels to optimize the performance of the controller. Simulation results show that the simplicity of the design and implementation of the control strategy do not compromise its performance thus providing a better trade-off than other similar and commonly-used solutions, at least in the considered scenarios. Results also show that the proposed controller is effective for any kind of storage technology, regardless of their specific features such as response time, and power and energy capacities.

2. **Secondary Frequency Control**
    - The participation of slow CI-ESSs such as BESs in the secondary frequency control of a power system (i.e., the AGC) leads to a statistical reduction of the spread of the frequency variations of a system subject to, e.g., stochastic wind and/or load variations. One must also consider that, when the BES device participates in the AGC, the magnitude of the variations of its state of charge increases. This implies a more frequent use of the storage device, increasing the number of charge/discharge processes, thus reducing to some extent its operational life. Whether or not an energy storage device should be included in the AGC is a trade-off between the

impact on the dynamic behavior of the grid and the aging of the storage device itself.

3. Transient Stability

- From the transient stability point of view, similar results were obtained when the CI-ESS regulates the frequency of the center of inertia (global) and the frequency at the bus of connection (local). In the case of the AIITS, results show a reduction of the probability of losing synchronism for a given critical clearing time (CCT) associated with a short-circuit of up to 20% in the case of fast CI-ESSs, and 15% for slow CI-ESSs.
- The reactive power support of the CI-ESS plays the major role in transient stability enhancement, i.e., the increase of the CCTs. Sustaining the voltage during the fault, in fact, reduces the probability that synchronous machines lose synchronism. Therefore, it is recommended to install CI-ESSs with relatively high reactive power rates.
- Different locations of the CI-ESS with respect to the fault and a synchronous machine have also been studied. If the fault occurs between the synchronous machine and the CI-ESS, the support provided by the latter is substantially diminished. This result is due to the closer location of the fault with respect to the synchronous machine, and to the barrier effect that the fault creates between the machine and the ESS, limiting the support provided by the latter.
- A STATCOM device outperforms the CI-ESS in some scenarios. One would expect that the CI-ESS, in the worst case, performs as well as a STATCOM device. However, this is not always the case, especially when the BES regulates the local bus frequency. If the dynamic response of the storage device and/or of its controller is not sufficiently fast (as in the case of the BES), the overall performance of the CI-ESS can be less effective than the STATCOM alone. Current limits of the power converter also increase the risk of instability. Fast, large transients such as three-phase faults may require a large reserve of active power to be supplied/absorbed by the storage device very quickly, increasing the risk of saturation of the CI-ESS, and therefore, reducing the CCT.

4. Voltage Stability

- Simulation results indicate that the inclusion of fast-responding reactive power support improve every aspect of the voltage stability studied as it: (i) increases the maximum loading level of the system; (ii) improves the small-signal stability for large loading conditions; (iii) reduces voltage oscillations due to perturbations such as those caused by the wind; (iv) maintains the voltage at the bus of connection at its reference value for a variety of disturbances, and (v) reduces the voltage sag resulting from large disturbances such as line outages and faults.
- Other less intuitive results have also been observed: (i) CI-ESSs provide more efficient voltage regulation than other solutions such as STATCOM devices thanks to their capability to provide simultaneously active and reactive power support; (ii) the dynamics of the energy storage device and its active power control do not deteriorate the small-signal voltage stability of the system even for large loading levels; (iii) current saturations of the power converter do not appear to compromise the short-term voltage stability of the overall system, at least in the considered scenarios; (iv) the impact of the local voltage support provided by CI-ESSs can be observed at a system level.

3.4 Frequency Control of Grid-Connected Microgrids

The bulk of papers [18, 19, 20, 21, 22] discuss the potential impact on frequency control of microgrids (MGs). A detailed summary of such discussions has been provided in deliverable D2.6. Based on all simulation results, the following remarks and recommendations are relevant.

- Without a proper control, MGs can contribute to destabilize the system. In particular, if the MGs only aim at maximizing their revenues, their impact on the system unbalance can be significant [18].
- The effect of the size of the energy storage systems (ESSs) included in the MGs is somewhat counterintuitive. If the MGs aims at maximizing their revenues, then the higher the size of the ESS, the higher is the negative impact on the frequency stability of the system [19, 20]. This is consistent as, the higher the capacity of the ESS, the more the MGs are able to "take advantage" of the market, waiting for the right moment to sell energy, i.e., when the electricity price is high, or storing it when the electricity price is low. Small ESSs, on the other hand, makes the MGs more dependent on the system and prone to suffer the stochastic behavior of their renewable energy resources and loads.
- The best approach to control the frequency through the MGs is a fully decentralized control. The work carried out in [22] clearly shows that the Additive Increase Multiplicative Decrease (AIMD) algorithm that has been originally developed for internet connections, is also very effective for MGs. The AIMD approach allow the MGs to both maximize their revenue and provide frequency support to the grid. Interestingly, this algorithm works better with a high number of "agents" (the MGs in this case) and, thus, intrinsically scales very well. Another relevant feature of the AIMD algorithm is that absolutely no communication at all is needed among the MGs and between the MGs and the system.
- If an AIMD approach to regulate the frequency is adopted, the impact of the ESSs included in the MGs is higher the higher the capacity of the ESSs themselves [21]. The benefit, however, is not linear and tends to show a saturation. This means that there is an optimal value of the capacity of the ESS beyond which the MG does not get any significant additional economical benefit from the ESS. Interestingly, the ESS capacity that is beneficial to the grid in terms of frequency control also saturates, but not at the same value for which it does with respect to the economical benefit for the MGs. This means that MGs might or might not need incentives to install bigger ESS. This depends on several factors, including: network size and topology, loading condition, and number of MGs and conventional generation included in the system.

From the conclusions above, it appears that the implementation of an *ad hoc* ICT system to communicate among MGs or to connect MGs to the grid is not recommended, at least for what concerns primary frequency control. On the other hand, each MG has to coordinate the devices, namely, renewable generators, storage, load, included in the MG itself. This is done through the Energy Management System (EMS) (see for example [18] and [20]). Typical MGs are relatively small both in terms of energy capacity and spatial dimensions. It is thus auspicious that the EMS is implemented with an efficient and reliable communication system.

4. Drafting of Ancillary Services and Network Code Definitions for the Provision of Primary and Secondary Frequency Control

This chapter is intended to update the new power-frequency control concepts with case studies on the Romanian power system database. The detailed principles of the two automatic frequency control levels in operation today, namely primary and secondary frequency control, have been presented in deliverables D2.1 and D2.2, while a first version of the new concepts promoted in this deliverable was presented in deliverable D2.6. This deliverable extends the theoretical aspects presented in deliverable D2.6 with more details of the control schemes and the results of the simulations. Based on the simulation results, we draw appropriate conclusions and make recommendations to the list of the proposed NCs and ASs.

The simulations are focused on the use of CI-ESSs in three power-frequency control levels, i.e.:

- Frequency Containment Control (FCC) – also referred to as PFC,
- automatic Frequency Restoration Control (aFRC) – also referred to as SFC, and
- Virtual Power Plant (VPP) control.

The purpose is to determine the effectiveness of the control strategies currently applied, and to compare them with the improved solutions based on the extensive use of CI-ESSs. Additionally, conclusions regarding the use size of the CI-ESSs in relation to the requirements for ensuring the minimum control capability in a certain power system to ensure frequency stability under the most critical operating conditions.

The technical solutions that we promote in this project may require adaptations in terms of market structure, responsibilities of the involved actors, and advancements in several types of technology. For this reason, when necessary, our technical solutions are completed with administrative and economic recommendations, without getting into details.

4.1 Primary Frequency Control

4.1.1 The General Framework

As mentioned in D2.1, D2.2 and D2.6, the primary frequency control is an independent and automatic control action, currently provided by all synchronous generation units connected to the grid. Therefore, the input signal to the regulator is the rotor angular speed of the synchronous generator, which is then compared to the reference value. The droop control technique is then usually employed to determine the equivalent power required to the provided in response to frequency variation. Such approach does not require special or complex power system architectures, but reliable and effective control resources.

A minimum frequency containment reserve must be maintained in each power system determined according to the total maximum load that can be recorded in the interconnected power system. Currently, the power system operator relies mostly on the large power plants and on the advantage provided by the wide synchronous interconnection which helps maintaining the frequency within tight limits almost all the time. However, as the large and reliable synchronous power plants are replaced with small and intermittent non-synchronous renewable energy sources, ensuring a deterministic frequency containment reserve is a challenge for the system operator. The reserves should be planned for both upwards and downwards power control.

The FCC comes after the instant reaction of the synchronous machines that naturally provide kinetic energy to counteract transient phenomena. Until now, a faster intervention of the FCC was not necessary because of the large mechanical inertia and kinetic energy available in classic power plants. On the other hand, we have to note that the FCC of conventional power plants are not capable in intervening faster than a few seconds from the identification of the perturbation.

4.1.2 Discussion of Results and Recommendations

Based on the simulations performed on the Romanian power system database in both Eurostag (please see Appendix B of this deliverable) and Simulink (please see deliverables D2.2 and D5.7), the following remarks and recommendations are relevant:

- In low-inertia power systems, the hydro units are not capable of stabilizing the frequency. Furthermore, because of their construction, some hydro units have an inverse effect in the first instants after the unbalance inception which amplifies the instability. For this reason, faster units are necessary, e.g. electrochemical CI-ESS, super-capacitors, flywheels.
- A new component should be introduced within the balancing market called fast frequency containment control (FFCC). As duly discussed in Chapter 3, FFCC can be based on fast-responding devices such as CI-ESSs and RESs. However, the need for this market component have to be decided for the whole Continental system of ENTSO-E based on detailed simulations of the entire ENTSO-E system database. The reserves and the type of technology (characterized by response time) needed for such a control should also be based on detailed simulations of the most severe perturbations.
- A minimum level of power reserve should be available in fast-acting resources. This level depends on the share of mechanical inertia available in synchronous generators and their location within the system. In transient state, the power rating is more important than the energy capacity. In order to maintain the system stability, it is not necessary to design a power reserve capable of recovering the frequency very close to the nominal value. This is because this control level should be designed to ensure the frequency stability, while the slow FCC can take the next steps in recovering the frequency. Note that, these aspects can involve economic discussions.
- The future grid code related to the CI-ESSs should define the economic aspects related to the automatic FCC.
- If conventional, decentralized FCC is applied, no communication is necessary with external entities. All hardware systems required for the FCC are available on-site, as components of the metering and automation systems of each generation resource. This control approach is robust because it does not depend on other systems but reacts to local signals.
- For the best results, it is recommended that the FCC reserves are uniformly located within the power system. This avoids large excursions of power flows over long distances.
- Standardized operation characteristics should be provided for those units that respond to both inertial and frequency containment control. This is important because the two actions are linked in time, and the power provided as frequency control service is set eventually by the same controller.

4.2 Secondary Frequency Control

4.2.1 The General Framework

The aFRC is activated in order to restore the FCR so that, at any instant, a larger fast acting power reserve is available to correct rapid frequency variations within the system. Additionally, aFRC is designed to cancel the frequency deviation and bring the system frequency back to the reference value. This will indirectly restore the net power interchange to the scheduled value.

Some power systems rely on hydro-generators and/or large turbo-generators. The power systems relying mostly on turbo-generators are subjected to significant changes in order to ensure the internal balance of the active power. These solutions depend on the technology development and the power market structure. Inter-TSO support can also be considered.

As the aFRC is a slow action, there is a wider freedom for qualifying other types of energy resources in case that the resources available in classical power plants are no longer available. In order to

ensure a predictability of these resources, the aggregation of resources of various characteristics are operated in such a way to be seen by the power market operators as a single entity. Such aggregations are the VPP, and the MG. An aggregation may not necessary be limited to generation entities, but also can include flexible loads and CI-ESSs.

The VPP is seen as any other power plant by the AGC, which means that a control signal is sent to the VPP controller. The VPP consists of any type of intermittent sources, CI-ESSs and hydro units. Usually, intermittent sources are not involved in providing secondary frequency control because their stochastic behavior. Only hydro units and CI-ESSs participate in the aFCR. A VPP is created to cancel the fluctuations in power generation of the intermittent sources. The main idea is to use deterministic type sources to balance the intermittent sources.

More details on the structure of the secondary frequency control level are found in deliverable D2.2.

4.2.2 Discussion of Results and Recommendations

Based on the simulations performed on the Romanian power system database in both Eurostag and Simulink, the following remarks and recommendations are relevant:

- The VPPs and the MGs will play an active role in the secondary frequency control. Both concepts can be classified as aggregators. A VPP is a coordinated group of generation units and loads located in different parts of the national network. The MG is a coordinated group of generation units and loads located in the same local network. Both types of aggregators require standardization of the operation in relation to the network operator in the grid cods, such as: communication type, reserve monitoring and Quality of Service (QoS) monitoring.
- A central controller is required for both VPP and MG. There must be a communication channel between the AGC and the VPP controller. For logistic reasons, the VPP controller can be better located in a city. The VPP controller can be seen as a power plant controller that distributes the signal received from the central AGC to the individual generation units. However, in the case of a VPP, there must also be an internal balancing that eventually causes the central AGC to react.
- Using a CI-ESS within the aFRC can be an effective technical solution. However, long term analysis for multiple scenarios should be studied. This is because once the state of charge is low, the CI-ESS is no longer available to participate in case of under-frequencies, and has to wait for a load valley or surplus of power from renewables to charge. Therefore, large rated CI-ESSs should be considered in the aFRC to cover large power unbalances.
- When a CI-ESS is used for aFRC, delays should be added to the reaction of the CI-ESS in order to avoid the frequency to be restored in a longer time. The CI-ESS can be effectively used in various control levels by appropriately choosing the delay times.
- In order to save the energy available for aFRC, some CI-ESSs can be included in the tertiary frequency control level. Therefore, faster reaction from the tertiary control reserves can be designed in order to optimize the use energy resources in all control levels. However, this requires a more intense activity from the system operator.
- As the share of RES increases, larger CI-ESSs are required. These can be split into smaller units and operated in an aggregated manner, or large individual units can be built.

5. Drafting of Ancillary Services and Network Code Definitions for the Provision of Inverter-based Frequency Control in 100% Non-synchronous Systems

The transition towards 100% RES is not as far-fetched as it seems. According to [14], by 2025, eight countries in Continental Europe (CE) will reach full hourly 100% RES penetration level. Due to the steadily increase in RES integration, power electronic converters are expected to replace Synchronous Generators (SGs) by constituting the backbone of future power grids, except in cases of hydro power and biomass plants where synchronous generators are used.

The loss of SGs together with their mechanical inertia and their frequency control mechanisms, brings new challenges concerning power system stability and ability to maintain synchronism. The so-called grid-forming control strategies for converters are needed to address these challenges by replicating synchronous generators functionalities. However, SG emulation has the drawback of nonlinear swing dynamics. In this regard, the Linear Swing Dynamics (LSD) concept is proposed to exploit the smartness and controllability of power electronic converters to not only secure the operation of future power systems but also enhance their dynamic behavior.

This chapter discusses briefly the proposed solutions for systems with 100% converter-interfaced RES i.e. wind and solar power plants and the new forms of ASs provision with highlighting the need for new NC definitions.

5.1 Frequency Control of RES-tied Converters in Zero Inertia Power Grids

Replacing SGs, whose rotating masses contribute to the overall system inertia, by converter-driven RES results in weak power systems with zero mechanical inertia. The power system inertia defines the ability of the system to oppose changes to the frequency directly after a disturbance and helps minimize the RoCoF of the system. Hence, giving valuable time for the release of the frequency containment reserves. The absence of system inertia jeopardizes the power system stability.

As a result, future power systems will undergo radical changes in terms of system dynamic behavior, control, and operation. Therefore, new roles need to be defined for RES-tied converters as grid-forming converters.

Grid-forming converter control enables grid operation in the absence of SGs by achieving synchronism and setting the voltage and angle reference of the power system. It has been used in small systems i.e. microgrids. However grid-forming converters would need to be applied on broader scales for future scenarios of 100% RES or even at country levels to ensure secure system operation in case of system split or islanded operation [16].

Different grid-forming converter control strategies are proposed in the literature to deal with the lack of system inertia and emulate the functionalities of SGs such as the Virtual Synchronous Generator (VSG), which is considered in the RESERVE project for validating the proposed concepts for frequency control in 100% non-synchronous systems.

As specified in Chapter 5 of deliverable D2.6, the frequency control of current power systems is defined by the ENTSO-E [13] to have a hierarchical architecture including primary, secondary, and tertiary frequency control with clear time-scale separation. As for the inertial response of current power systems, it is an inherent response of the SGs, naturally released following any power imbalance. However, in future power grids, with up to 100% converter-based RES, the inertial response, in addition to the active power reserves, would need to be provided by means of ESSs.

Moreover, power electronics, in contrast to rotating masses, can have very fast responses and so the control time frames will be reduced and the frequency control hierarchy will disappear. Therefore, frequency control with reduced time frames such as fast primary control and distributed secondary control are proposed.

5.1.1 Distributed Secondary Frequency Control

One of the goals of secondary control is to restore the frequency back to the nominal value after a power unbalance. The secondary control is centralized in conventional power systems and usually involves the transmission level. At this level, the communication takes place between the control center and the power plants providing secondary reserve, with a control time frame from 30 seconds up to 15 minutes. The long time frame is due to the centralized control architecture and the fact that SGs cannot change their settings and output power so fast.

In the wake of the increased integration of inverter interfaced-RES, the communication among the converters can be leveraged to enhance the performance of secondary frequency control, achieve faster frequency restoration and overcome reduction in reliability as in the conventional centralized approach. This concept of distributed secondary control has already been used for microgrids and it might be as well considered in the future for 100% non-synchronous system since the response speed of inverter-interfaced RES is much faster than SGs.

The distributed control approach is mainly based on consensus algorithms. In the RESERVE project, the distributed averaging-based integral (DAI) control [54], which only requires local frequency measurement and neighborhood communication, is considered. The advantages of this approach are that it eliminates the steady state frequency error and it achieves optimal solution for the economic dispatch problem. In practice, communication channels between converters will suffer from communication latency and noise, which will affect the performance and stability of the distributed secondary controllers. Hence, different test scenarios for distributed frequency control with noise and time-delays have been considered as part of the case study presented in Appendix C.1.3.1.

5.2 Linear Swing Dynamics for Converter-Based Power Grids

The aforementioned VSG converter emulates the SG based on the classical representation of the nonlinear swing equation. However, future power systems do not need to be defined based on legacy systems, instead, with the degrees of freedom introduced by power electronics, it is possible to shape and enhance the system dynamic behavior. Hence, the LSD concept [46] has been introduced and adopted in the development of SG emulation in the VSG. The LSD-based VSG (LSD-VSG) proposes a smart and grid-friendly converter that emulates the classical SG but with linearized power-angle characteristics. This in turn results in simplified modal and stability analysis of future power systems. The LSD concept has been introduced in deliverable D2.3 for the single machine infinite bus case, more details on the decentralized LSD concept for multi-machine systems are represented in Appendix C.1.2.

5.3 Frequency Control of HVDC Systems Connecting Low/ Zero Inertia Power Grids

According to the ENTSO-E Ten Years Network Development Plan (TYNDP), for 2030 there will be more than 140 HVDC projects in service, under construction or commissioning in Europe [17]. This emphasizes the significant futuristic role of HVDC systems in their participation to frequency stabilization of future electrical networks.

This deliverable presents the two innovative control solutions for HVDC systems: the Multi-Agent based Intelligent Frequency Control (MA-IFC) [38], and LSD-VSG [37]. The two schemes are developed and implemented in grid-tied HVDC converters to define a new role and behavior for HVDC systems in frequency stabilization of AC grids. Comprehensive tests scenarios are conducted to further validate the proposed solutions and provide coherent conclusions regarding recommendations to new NCs for HVDC connection.

The MA-IFC scheme is tested and compared with the well-known Frequency Droop Control (FDC), considering different test scenarios. Results are provided in Appendix C.2.1.

The LSD-VSG is tested and compared with the recently proposed VSG to show that the former has

a better performance in terms of:

1. Enhancing DC voltage profile; and
2. achieving linear power-angle characteristics in the HVDC converters.

Note that achieving LSD (power-angle linearization) relies on AC voltage control, by exploiting the permitted AC voltage tolerance. Hence, a difference in AC voltage profile is observed with LSD-VSG comparing with classical VSG.

Since both schemes use active power-frequency droop control loop, a similar frequency profile is obtained as shown in the results in Figure C.19.

5.4 Discussion of Results and Recommendations

The performance evaluation and the validation of the proposed solutions, for which conclusions and new NC recommendations will be drawn, have been carried out through comprehensive simulations on the WSCC 9-bus system. Relevant simulation results are presented in Appendix C.

1. DAI control

- The results show that the proposed distributed secondary control strategy at transmission level shows a good performance in restoring the system nominal frequency.
- The DAI control is scalable and only requires sparse communication. Hence, it is more reliable in comparison to the centralized approach.
- The DAI control has shown good robustness and performance under noise as well as communication delays up to 200 ms as shown in Figures C.3 and C.4. However, larger delays increase the oscillations in the frequency and could destabilize the system. Hence, fast communication would be needed.
- In transmission systems, due to long geographical distances, fiber optic links would be used for communication.

2. LSD-VSG

- The LSD-VSG has better performance in terms of RoCoF and frequency nadir as shown in Figures C.10 and C.12.
- The LSD (power-angle characteristics linearization) is achieved through voltage control. Hence, the LSD-VSG offers P-V control but not Q-V control.
- The developed LSD-VSG control is decentralized i.e. there is no coordination nor communication between the converters. Only the network topology is needed for calculating the Thevenin equivalent impedance used in the LSD control law as explained in Appendix C.1.2. However, as depicted in Figure C.8, the lack of information following a topology change does not affect the stability of the LSD-VSG converter.

3. LSD for Converter-Based Power Grids

- The grid-forming converters (VSG and LSD-VSG) are capable of managing the operation of the power system, under both normal operation and disturbances, without the need for SGs to support the system.
- The parameters (inertia constant and damping) of the VSG and LSD-VSG virtual inertia control loop, can be tunable. The inertia constant is mainly based on the energy of the ESS connected the converter's DC link, while the damping is a free parameter. Simulation results have shown that larger damping values result in smaller RoCoF as depicted in Figure C.10.a, but very large values could destabilize the system as shown in Figure C.9. In future power systems, the system stability and performance will rely thoroughly on the control of the converters, hence,

the control parameters should be coordinated by the TSO according to the desired system performance metrics i.e. RoCoF and frequency nadir following a contingency.

- Due to the fast response of the converter-interfaced RES as shown in Figure C.5.a, reduced time frame for system operation and control is needed. This also includes the RoCoF measurement time window. According to the guideline [47], the RoCoF calculation window is 250 ms. However, given the fact that grid-forming converters introduce faster dynamics, the TSO needs to specify a smaller RoCoF calculation windows to deal with the converters fast transients.
- The droop settings according to the ENTSO-E [15] should be between 2% and 12%. However, high droop settings result in deteriorated frequency performance metrics (i.e. large RoCoF and frequency nadir) as shown in Figure C.12, in addition to power oscillations as shown in Figure C.11.b. Hence, as with the virtual inertia control loop parameters, the TSO needs to coordinate the droop settings according to the desired frequency metrics and power sharing between different converters.

4. HVDC – MA-IFC Scheme

- The control setting, including frequency droop coefficient, should be changed by time based on: instantaneous generation and demand, technical specifications and constraints (e.g. existing inertia and damping) of each AC grid connected to HVDC systems. Control setting means deciding the amount of active power participation (injection) by healthy AC grids to provide frequency support to the disturbed AC grid. This should be done in coordination with HVDC owners and respective transmission system operators.
- The communication among the controllers (HVDC converter stations) will be likely done via fiber optic cables. It is worth mentioning that the MA-IFC scheme has shown robust performance under agent failure as well as communication delay as shown in Figures C.16–C.18 in Appendix C.2.1.
- The MA-IFC is scalable for any future network extension, and it is viable for all HVDC-connected AC grids, including weak and island AC grids.

5. HVDC – LSD-VSG

- The grid-tied HVDC converters are recommended to operate with a new form of Synchronous Generator (SG) emulation based on LSD concept. This fulfills the futuristic requirements of both DC system and connected AC grids as follows:
    - Active power delivery, as a main role for HVDC systems, while maintaining a stable operation and regulated DC voltage profile; and
    - participation in grid frequency stabilization while contributing in shaping linear and uniform system swing dynamics of respective (connected) AC grids.

  Also, the new form of LSD-based SG emulation will enable the deployed HVDC converters to strengthen the synchronous connection among the HVDC-connected AC grids (European transmission networks)
- HVDC systems (converters) should be allowed to tolerate AC voltage within the permitted margin, i.e. 5% of nominal AC voltage, in order to achieve linear power-angle characteristics.
- Control actions are done with local measurements, i.e. there is no need for coordination and communication with other HVDC converter stations.

6. Concluding Remarks and Future Work

This deliverable concludes Task T2.6, and proposes a thorough list of recommendations for updates and creation of ancillary services and network code definitions concerning frequency control.

After a thorough review of the existing network codes and white papers that are currently under review at European level, and based on the results of the studies carried out in WP2 since the beginning of this project, we have identified a number of concepts that need to be carefully revised in such existing codes in order to take into account the participation of new agents into the different layers of the frequency control. These new agents include, but are not limited to, converter-interfaced energy storage systems, converter-interfaced generation, flexible loads, grid-connected microgrids and virtual power plants. On the other hand, the frequency control layers that have been considered in this deliverable are: (i) rate of change of frequency control and fast droop frequency control provided by converter-interfaced distributed energy resources, (ii) conventional primary frequency control provided by the synchronous power plants remaining in the system, and (iii) secondary frequency control with the participation of synchronous power plants as well as aggregated distributed resources in the form of virtual power plants. Moreover, two main scenarios have been considered, namely, (i) systems with a certain share of synchronous machines still connected to the system, and (ii) systems with 100% non-synchronous renewable energy sources.

The conclusions and recommendations proposed in this work have been evaluated, harmonized and promoted for international adoption by WP6, particularly in Deliverable D6.4.

Beyond the completion of this Task and, subsequently, of this project, we have identified a number of areas worthy of further investigation.

On one hand, the aggregation of distributed energy resources into virtual power plants appears to be a promising and, at the same time, challenging alternative to conventional power plants. From a system perspective, it is important to assess the interaction of such virtual power plants with the grid and the impact of different control strategies on the frequency stability of the overall power system. Several challenges can be identified, among which we cite:

1. The coordination of the resources available in the virtual power plant is complicated by the fact that such resources are distributed in the network and can possibly be located at several kilometers from each other. An efficient and properly setup communication system is thus required.

2. The control of each distributed resource has to be defined in a consistent and coordinated manner. This can be difficult if the resources that compose virtual plant have different owners.

3. To date, it is still highly unclear what is the best approach for the control of virtual plants, especially for the frequency support of the grid. From a purely control point of view, a centralized approach is certainly to be preferred. However, the need of a fast response, especially for the inertial response, may prevent a fully centralized approach. A decentralized control is also to be preferred for scalability as well as economic reasons.

4. Finally, the stochastic nature of most renewable sources further complicates the regulation as the power reserve for the frequency regulation is not a deterministic resource as in conventional power plants.

On the other hand, the linear-swing dynamics concept developed within WP2 can be extended in several ways. While some of the RESERVE products have reached maturity where they may be brought to market, others have been fostering the birth on new lines of research. This is the case with the LSD concept. With this game-changing concept we are able to integrate RES based on linear control theory so at the device-level we keep the problem as simplified as possible, yet at the system-level we can still tackle the power unbalance problem. The LSD research activities started within RESERVE were focused on frequency stability, however, transient stability and behaviour under faults will be further investigated in the future. Additionally, the LSD have spawned poten-

tial for further research considering voltage stability, since the presented LSD scheme integrates voltage control.

Finally, we remark the usefulness and versatility of the frequency divider formula developed throughout WP2. The numerous applications of the formula that have been developed and validated in the project, and which apply to a broad spectrum of areas such as modeling, control and state estimation, can be extended to other areas, for example, harmonic analysis. However, despite the abundant contributions of the frequency divider formula that have been discussed so far, it seems that only the surface has been scratched. We think that, in the long term, the formula can help rewrite the selfsame power system theoretical foundations.

7. List of Figures

8. List of Tables

9. References

[1] H. Asano, K. Yajima, and Y. Kaya. Influence of photovoltaic power generation on required capacity for load frequency control. *IEEE Transactions on Energy Conversion*, 11(1):188–193, March 1996.

[2] I. Beil, I. Hiskens, and S. Backhaus. Frequency regulation from commercial building HVAC demand response. *Procs of the IEEE*, 104(4):745–757, April 2016.

[3] P. Bhui, N. Senroy, A. K. Singh, and B. C. Pal. Estimation of inherent governor dead-band and regulation using unscented Kalman filter. *IEEE Transactions on Power Systems*, 33(4):3546–3558, July 2018.

[4] J. Boyle, T. Littler, and A. Foley. Review of frequency stability services for grid balancing with wind generation. *The Journal of Engineering*, 2018(15):1061–1065, 2018.

[5] M. Cheng, J. Wu, S. J. Galsworthy, C. E. Ugalde-Loo, N. Gargov, W. W. Hung, and N. Jenkins. Power system frequency response from the control of bitumen tanks. *IEEE Transactions on Power Systems*, 31(3):1769–1778, May 2016.

[6] Salvatore D'Arco, Jon Are Suul, and Olav B. Fosso. A Virtual Synchronous Machine implementation for distributed control of power converters in SmartGrids. *Electric Power Systems Research*, 122:180–197, 2015.

[7] P. Du and Y. Makarov. Using disturbance data to monitor primary frequency response for power system interconnections. *IEEE Transactions on Power Systems*, 29(3):1431–1432, May 2014.

[8] P. Du and J. Matevosyan. Forecast system inertia condition and its impact to integrate more renewables. *IEEE Transactions on Smart Grid*, 9(2):1531–1533, March 2018.

[9] EirGrid and SONI. All-island ten year transmission forecast statement 2017, 2018. URL `http://www.eirgridgroup.com/site-files/library/EirGrid/TYTFS-2017-Final.pdf`.

[10] EirGrid Group. All island Irish transmission system map. URL `http://smartgriddashboard.eirgrid.com/#all/transmission-map`.

[11] A. Elrayyah, Y. Sozer, and M. E. Elbuluk. Modeling and control design of microgrid-connected PV-based sources. *IEEE Journal of Emerging and Selected Topics in Power Electronics*, 2(4):907–919, December 2014.

[12] J. H. Eto, J. Undrill, P. Mackin, R. Daschmans, B. Williams, B. Haney, R. Hunt, J. Ellis, H. Illian, C. Martinez, M. O'Malley, K. Coughlin, and K. Hamachi LaCommare. Use of frequency response metrics to assess the planning and operating requirements for for reliable integration of variable renewable generation. Technical Report LBNL-4145E, Lawrence Berkeley National Laboratory, Berkeley, 2010.

[13] European Network of Transmission System Operators for Electricity (ENTSO-E). Supporting Document for the Network Code on Load-Frequency Control and Reserves, 2013.

[14] European Network of Transmission System Operators for Electricity (ENTSO-E). Scenario Outlook & Adequacy Forecast 2015, June 2015.

[15] European Network of Transmission System Operators for Electricity (ENTSO-E). Guideline on Electricity Balancing, 2016. Commision Regulation (EU) 2016/1719.

[16] European Network of Transmission System Operators for Electricity (ENTSO-E). High Penetration of Power Electronic Interfaced Power Sources (HPoPEIPS), March 2017.

[17] European Network of Transmission System Operators for Electricity (ENTSO-E). TYNDP 2018 Executive Report – Connecting Europe: Electricity – 2025 - 2030 - 2040. Technical report, 2018. URL `https://tyndp.entsoe.eu/`.

[18] P. Ferraro, E. Crisostomi, M. Raugi, and F. Milano. Analysis of the impact of microgrid penetration on power system dynamics. *IEEE Transactions on Power Systems*, 32(5):4101–4109, September 2017.

[19] P. Ferraro, E. Crisostomi, M. Raugi, and F. Milano. Decentralized stochastic control of microgrids to improve system frequency stability. In *Proceedings of the IEEE PES Innovative Smart Grid Technologies Conference Europe (ISGT-Europe)*, pages 1–6, Torino, Italy, September 2017.

[20] P. Ferraro, E. Crisostomi, M. Raugi, and F. Milano. On the impact of microgrid energy management systems on power system dynamics. In *Proceedings of the IEEE PES General Meeting*, pages 1–5, Chicago, IL, July 2017.

[21] P. Ferraro, E. Crisostomi, and F. Milano. Evaluation of the impact of the size of storage devices in grid-connected microgrid. In *Proceedings of the IEEE PES International Conference on Environment and Electrical Engineering (EEEIC)*, pages 1–6, Palermo, Italy, June 2018.

[22] P. Ferraro, E. Crisostomi, R. Shorten, and F. Milano. Stochastic frequency control of grid-connected microgrids. *IEEE Transactions on Power Systems*, 33(5):5704–5713, Sept 2018.

[23] V. Gevorgian, Y. Zhang, and E. Ela. Investigating the impacts of wind generation participation in interconnection frequency response. *IEEE Transactions on Sustainable Energy*, 6(3):1004–1012, July 2015.

[24] M. Guan, J. Cheng, C. Wang, Q. Hao, W. Pan, J. Zhang, and X. Zheng. The frequency regulation scheme of interconnected grids with VSC-HVDC links. *IEEE Transactions on Power Systems*, 32(2):864–872, March 2017.

[25] International Renewable Energy Agency (IRENA). Battery storage for renewables: Market status and technology outlook, 2015. URL `www.irena.org/-/media/Files/IRENA/Agency/Publication/2015/IRENA_Battery_Storage_report_2015.pdf`.

[26] N. Kakimoto, S. Takayama, H. Satoh, and K. Nakamura. Power modulation of photovoltaic generator for frequency control of power system. *IEEE Transactions on Energy Conversion*, 24(4):943–949, December 2009.

[27] G. Kron. *Tensor Analysis of Networks*. Wiley, Hoboken, NJ, USA, 1939.

[28] Market Observatory for Energy. Quarterly report on European electricity markets. Technical Report vol. 11, no. 3, European Comission, 2018. URL `https://ec.europa.eu/energy/sites/ener/files/documents/quarterly_report_on_european_electricity_markets_q3_2018.pdf`.

[29] F. Milano. Rotor speed-free estimation of the frequency of the center of inertia. *IEEE Transactions on Power Systems*, 33(1):1153–1155, Jan 2018.

[30] F. Milano and Á. Ortega. Frequency makers vs frequency takers – Part I: Theory and applications. *IEEE Transactions on Power Systems*. Submitted in February 2019 and currently under review.

[31] F. Milano and Á. Ortega Manjavacas. *Converter-Interfaced Energy Storage Systems – Context, Modelling and Dynamic Analysis*. Cambridge University Press, Cambridge, United Kingdom, 2019.

[32] F. Milano, F. Dörfler, G. Hug, D. J. Hill, and G. Verbič. Foundations and challenges of low-inertia systems (invited paper). In *Proceedings of the Power Systems Computation Conference (PSCC)*, pages 1–25, Dublin, Ireland, June 2018.

[33] F. Milano, Á. Ortega, and A. J. Conejo. Model-agnostic linear estimation of generator rotor speeds based on phasor measurement units. *IEEE Transactions on Power Systems*, 33(6):7258–7268, November 2018.

[34] Federico Milano and Álvaro Ortega. Frequency divider. *IEEE Transactions on Power Systems*, 32(2):1493–1501, March 2017.

[35] N. Monshizadeh, C. De Persis, A. J. van der Schaft, and J. M. A. Scherpen. A novel reduced model for electrical networks with constant power loads. *IEEE Transactions on Automatic Control*, 63(5):1288–1299, May 2018. ISSN 0018-9286. doi: 10.1109/TAC.2017.2747763.

[36] J. Morren, S. W. H. de Haan, W. L. Kling, and J. A. Ferreira. Wind turbines emulating inertia and supporting primary frequency control. *IEEE Transactions on Power Systems*, 21(1):433–434, February 2006.

[37] A. Musa, A. Kaushal, S. K. Gurumurthy, D. Raisz, F. Ponci, and A. Monti. Development and stability analysis of LSD-based virtual synchronous generator for HVDC systems. In *IECON 2018 - 44th Annual Conference of the IEEE Industrial Electronics Society*, pages 3535–3542, Oct 2018.

[38] Aysar Musa, Lorenzo Sabug, Ferdinanda Ponci, and Antonello Monti. Multi-agent based intelligent frequency control in multi-terminal DC grid-based hybrid AC/DC networks. *IET Renewable Power Generation*, 12(13):1434–1443, Oct 2018.

[39] Á. Ortega and F. Milano. Frequency makers vs frequency takers – Part II: Illustrative examples and case studies. *IEEE Transactions on Power Systems*. Submitted in February 2019 and currently under review.

[40] Á. Ortega and F. Milano. Modeling, simulation, and comparison of control techniques for energy storage systems. *IEEE Transactions on Power Systems*, 32(3):2445–2454, May 2017.

[41] Á. Ortega and F. Milano. Comparison of different PLL implementations for frequency estimation and control. In *Procs. of the 18th International Conference on Harmonics and Quality of Power (ICHQP)*, pages 1–6, May 2018.

[42] Á. Ortega and Federico Milano. Comparison of bus frequency estimators for power system transient stability analysis. In *Proceedings of the POWERCON Conference*, Wollongong, Australia, September 2016.

[43] Á. Ortega and Federico Milano. Impact of frequency estimation for VSC-based devices with primary frequency control. In *Proceedings of the IEEE PES Innovative Smart Grid Technologies Europe (ISGT Europe)*, Torino, Italy, September 2017.

[44] Álvaro Ortega and Federico Milano. Frequency control of distributed energy resources in distribution networks. In *Proceedings of the 10th IFAC Symposium on Control of Power and Energy Systems CPES 2018*, Tokyo, Japan, September 2018.

[45] A. Oudalov, D. Chartouni, and C. Ohler. Optimizing a battery energy storage system for primary frequency control. *IEEE Transactions on Power Systems*, 22(3):1259–1266, August 2007.

[46] D. Raisz, A. Musa, F. Ponci, and A. Monti. Linear and uniform system dynamics of future converter-based power systems. In *2018 IEEE Power Energy Society General Meeting (PESGM)*, pages 1–5, Aug 2018.

[47] RG-CE System Protection & Dynamics Sub Group. Frequency measurement requirements and usage. Technical report, European Network of Transmission System Operators for Electricity (ENTSO-E), 2018.

[48] K. Samarakoon, J. Ekanayake, and N. Jenkins. Investigation of domestic load control to provide primary frequency response using smart meters. *IEEE Transactions on Smart Grid*, 3(1):282–292, March 2012.

[49] J. W. Shim, G. Verbič, N. Zhang, and K. Hur. Harmonious integration of faster-acting energy storage systems into frequency control reserves in power grid with high renewable generation. *IEEE Transactions on Power Systems*, 33 (6):6193–6205, November 2018.

[50] B. Tamimi, C. Cañizares, and K. Bhattacharya. System stability impact of large-scale and distributed solar photovoltaic generation: The case of Ontario, Canada. *IEEE Trans. on Sustainable Energy*, 4(3):680–688, July 2013.

[51] Transelectrica. Avize/contracte pentru centralele eoliene. URL `http://www.transelectrica.ro/avize-contracte`.

[52] E. Vrettos, C. Ziras, and G. Andersson. Fast and reliable primary frequency reserves from refrigerators with decentralized stochastic control. *IEEE Transactions on Power Systems*, 32(4):2924–2941, July 2017.

[53] Rafael Zárate Miñano and Federico Milano. Construction of SDE-based wind speed models with exponentially decaying autocorrelation. *Renewable Energy*, 94:186 – 196, 2016.

[54] C. Zhao, E. Mallada, and F. Dörfler. Distributed frequency control for stability and economic dispatch in power networks. In *2015 American Control Conference (ACC)*, pages 2359–2364, July 2015.

[55] J. Zhao, L. Mili, and F. Milano. Robust frequency divider for power system online monitoring and control. *IEEE Transactions on Power Systems*, 33(4):4414–4423, July 2018.

10. List of Abbreviations

AC	Alternating Current
ACE	Area Control Error
aFRC	automatic Frequency Restoration Control
aFRR	automatic Frequency Restoration Reserve
AGC	Automatic Generation Control
AIITS	All-island Irish Transmission System
AIMD	Additive Increase Multiplicative Decrease
AS	Ancillary Service
ASM	Ancillary Service Market
AVR	Automatic Voltage Regulator
BDC	Bucharest Dispatch Centre
BES	Battery Energy Storage
BES	Battery Energy Storage System
CACM	Capacity Allocation and Congestion Management
CAES	Compressed Air Energy Storage
CAISO	California Independent System Operator
CCT	Critical Clearing Time
CE	Continental Europe
CI-ESS	Converter-Interfaced Energy Storage System
CoI	Centre of Inertia
CPL	Constant Power Load
DAE	Differential Algebraic Equation
DAI	Distributed Averaging-based Integral
DAM	Day-Ahead Market
DC	Direct Current
DER	Distributed Energy Resource
DSO	Distribution System Operator
EMS	Energy Management System
ENTSO-E	European Network of Transmission System Operators for Electricity
EPEX	Centre-North European Power Market Exchange
E-PLL	Enhanced Phase-Locked Loop
ESS	Energy Storage System
EU	European Union
FCC	Frequency Containment Control
FCR	Frequency Containment Reserve
FDC	Frequency Droop Control
FDF	Frequency Divider Formula
FERC	Federal Energy Regulatory Commission
FES	Flywheel Energy Storage

FFCC	Fast Frequency Containment Control
HESS	Hybrid Energy Storage System
HIC	H-infinity Control
HPP	Hydro Power Plant
HV	High-Voltage
HVDC	High-Voltage Direct Current
ICT	Information and Communication Technologies
IEEE	Institute of Electrical and Electronics Engineers
IEM	Integrated European Market
IM	Intraday Market
IPEX	Italian Power Market Exchange
ISO	Independent System Operator
LMP	Locational Marginal Pricing
LPF	Low-Pass Filter
LPF-PLL	Low-Pass Filter Phase-Locked Loop
LSD	Linear Swing Dynamics
LSE	Load Serving Entities
MA-IFC	Multi-Agent-based Intelligent Frequency Control
mFRR	manual Frequency Restoration Reserve
MG	Microgrid
MPPT	Maximum Power Point Tracking
NC	Network Code
NDC	National Dispatch Center
NEMO	Nominated Electricity Market Operators
NYISO	New York Independent System Operator
ODE	Ordinary Differential Equations
PFC	Primary Frequency Control
PIC	Proportional Integral Control
PLL	Phase-Locked Loop
PMU	Phasor Measurement Unit
PV	Photo-Voltaic
QoS	Quality of Service
RES	Renewable Energy Sources
RoCoF	Rate of Change of Frequency
RoCoP	Rate of Change of Power
RR	Replacement Reserves
RTM	Real-Time Market
RTO	Regional Transmission Organizations

RTS	Romanian Transmission System
RWTH	Rheinisch-Westfälische Technische Hochschule
SCADA	Supervisory Control and Data Acquisition
SCES	Super Capacitor Energy Storage
SFC	Secondary Frequency Control
SG	Synchronous Generator
SMC	Sliding Mode Control
SMES	Superconducting Magnetic Energy Storage
SMIB	Single-Machine Infinite-Bus
SOGI-FLL	Second-Order Generalized Integrator Frequency-Locked Loop
SRF-PLL	Synchronous Reference Frame Phase-Locked Loop
STATCOM	Static Synchronous Compensator
TSO	Transmission System Operator
TYNDP	Ten Years Network Development Plan
UCD	University College Dublin
UPB	Politehnica University of Bucharest
USA	United States of America
VPP	Virtual Power Plant
VSG	Virtual Synchronous Generator
WP	Work Package
WSCC	Western Systems Coordinating Council

A. Frequency Estimation and Fast Frequency Control

A.1 Taxonomy of Frequency Takers and Frequency Makers

A.1.1 Frequency Takers

According to our definition, a frequency taker is a device for which the local frequency at the bus where the device is connected, $\Delta\omega_{\text{B},1}(t)$, is equal to the frequency of its neighboring bus (assuming a connection in antenna), $\Delta\omega_{\text{B},2}(t)$, as depicted in Figure A.1.

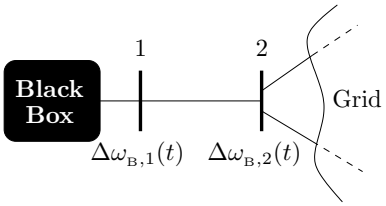

Figure A.1: Black-box device connected in antenna to the grid.

By construction of the FDF, there cannot be any variation of frequency within a passive circuit (boundary conditions on the frequency are imposed externally from the device). Constant power loads fall in this category. While analytically irreproachable, the condition $\Delta\omega_{\text{B},1}(t) = \Delta\omega_{\text{B},2}(t)$ is rarely satisfied in practice. We thus relax it and assume that a frequency taker is characterized by having variations of its injected/consumed active power over a given time window (i.e., its Rate of Change of Power or RoCoP) which are smaller than a given empirical threshold, ϵ. Once agreed upon by all parties, ϵ can be used by the TSO to define NCs and ASs. We further discuss on the numerical evaluation of this threshold in the two-part paper [30, 39].

Now, the condition to be a frequency taker can be satisfied in two cases, both relevant for our discussion:

- **Slow Power Variations:** The device does vary its power consumption/production, but the RoCoP is small in the considered time frame, i.e. the time scale of the primary frequency control. We have to expect, thus, that secondary frequency control or the daily ramp-up of loads do not actually vary the frequency at the buses.
- **Small Power Variations:** No load consumption or generation is ever perfectly constant. Stochastic white noise, at least, creates local tiny fluctuations. If the noise is small enough, however, such variations are unable impact on the frequency.

A.1.2 Frequency Makers

According to our definition, a device becomes a frequency maker whenever the RoCoP is larger than the defined ϵ. Following the discussion above, the only variations of power of interest are those that are sufficiently big to be able to actually vary the local frequency above a certain threshold and sufficiently fast to be comparable to the time scale of the inertial response and primary frequency control of synchronous machines. In the following, we consider various cases.

- **Synchronous Machines:** The variations of the active power generated by a synchronous machine depend on (i) the power set point as defined by the solution of the unit commitment problem; (ii) the regulating power due to primary frequency control (turbine governor) of the machine; (iii) the regulating power due to the secondary frequency control (automatic generation control, AGC) if any, and if the machine participates to it; and (iv) the inertial response of the machine. Of the four components above, the ones that actually contribute to modify the frequency at the machine bus and thus make the machine a frequency maker are the primary frequency control and the machine inertial response.

- **Non-synchronous device regulating the frequency:** In this category of devices we find, for example, grid-forming power electronics converters of wind turbines or energy storage systems, and thermostatically-controlled loads. We can thus assume that such devices are effectively a frequency control loop, with a given reference frequency. The actual implementation of the controller is unknown. However, whatever is the transfer function of the controller, it tracks the reference frequency. The particular case of wind turbines are worth discussing.

  The active power generated by a wind turbine depends on two factors, one due to the stochastic (uncertain and volatile) wind perturbation, and another which results from the frequency controller, if implemented. It is important to note that large and fast stochastic variations, such as wind gusts, are indistinguishable, in principle, from power variations aimed at regulating the frequency. The only difference is statistical. Wind gusts, in fact, will show, for about 50% of the times, a variation that further increases the actual frequency deviation with respect to the synchronous reference. Instead, a power variation imposed by a frequency controller, always aims at tracking the synchronous frequency. Wind gusts, however are relatively uncommon and typical values of the autocorrelation coefficients of wind speeds (see, for example, [53]) lead to conclude that wind turbulences have a small local effect on active power fluctuations, whereas the average value of the wind varies quite slowly with time. So, except for rare cases of strong wind gusts, the RoCoP of a wind turbine can be assumed to depend only on the response of the frequency regulator.

B. Primary and Secondary Frequency Control

B.1 Control Scheme of the BESS

In the simulations discussed in this Section, the ESS considered is a Battery Energy Storage System (BESS). The control scheme of the BESS consists of 3 loops (see Figure B.1):

1. The droop control loop, modeling the primary frequency control. This loop is based on the change in the frequency by comparing the system frequency, f_{sys}, with the reference frequency, f_{ref}. A deadband is used to avoid unnecessary contributions from the battery. The frequency variation value Δf is filtered out by using a low-pass filter (LPF), then amplified by a droop value, $K_{\Delta f}$. This control signal can be optional and can be enabled/disabled by means of the coefficient α_f.
2. The VPP loop. The battery is one of the main units that may be suitable for balancing the power generation of a VPP around the predefined value, which is an economic engagement of the VPP owner on the electricity market. Depending on technical and economic characteristics of all the VPP components, the battery system can produce or absorb more or less active power whenever there is an order from the VPP controller, especially to counteract strong intermittences. Long term and large unbalances can be handled by the VPP by considering other options, such as the hydro units. In Figure B.1, the power order received from the VPP controller is $P_{VPP\text{-}bat}$, whereas this option can be enabled or disabled by the coefficient α_{VPP}.
3. The secondary control loop. The storage system can receive a control signal, P_{AGC}, directly from the national AGC; this is optional in case that this signal is not sent via the VPP controller. This option can be activated in the simulation by means of the coefficient α_{AGC}.

The output power of the BESS, P_{BESS}, is limited to its power capacity in either direction, that is $P_{BESS}^{\min}$ and $P_{BESS}^{\max}$.

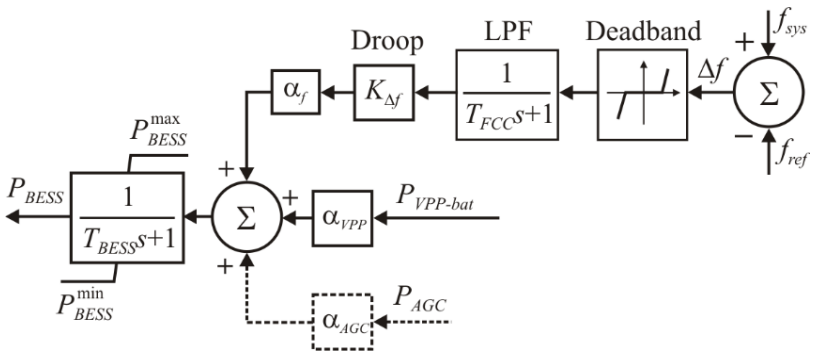

Figure B.1: Power and frequency control scheme of a storage system.

B.2 Control Scheme of the Virtual Power Plant

The VPP controller, depicted in Figure B.2, aims at setting the balancing control signals to be sent to the BESS and the hydro unit in order to satisfy the reference values. The VPP generation units can be located in different points of the electrical networks. For this reason, individual measurements should be performed. Power measurements from wind units, e.g. P_{w1}, P_{w2}, ..., P_{wn}, are inputs to the VPP controller, and the total wind power generation is filtered out to avoid reacting to very fast wind power spikes. The total power generation from wind, P_{VPP}, is compared to the VPP reference power, P_{VPPref}, decided by the VPP owner on the electricity market, as well as to the control signal received from the national AGC controller, P_{VPP_AGC}. The resulted error is passed through a PI regulator, whose output, ΔP_{VPP}, is introduced into a power repartition unit to determine the control setting of the hydro, P_{VPP_hyd}, and battery, P_{VPP_bat}, units associated to the VPP.

The PI regulator of the VPP should be faster than the PI regulator of the AGC in order to avoid unaccepted delays in frequency recovery within the secondary frequency control level.

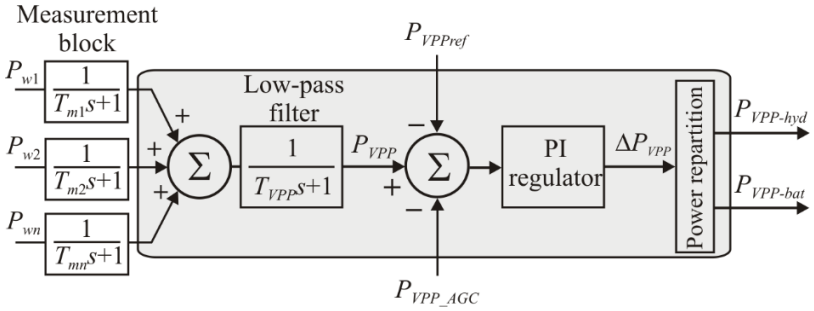

Figure B.2: VPP control scheme.

B.3 Central Automatic Generation Control

Figure B.3 illustrates the control scheme of the central AGC controller. As explained in deliverable D2.2, the central AGC operation is based on two types of measurements, i.e.:

- the active power flows (P_1, …, P_n) on the tie-lines
- the system frequency, f_{sys}, which is multiplied by a K-factor

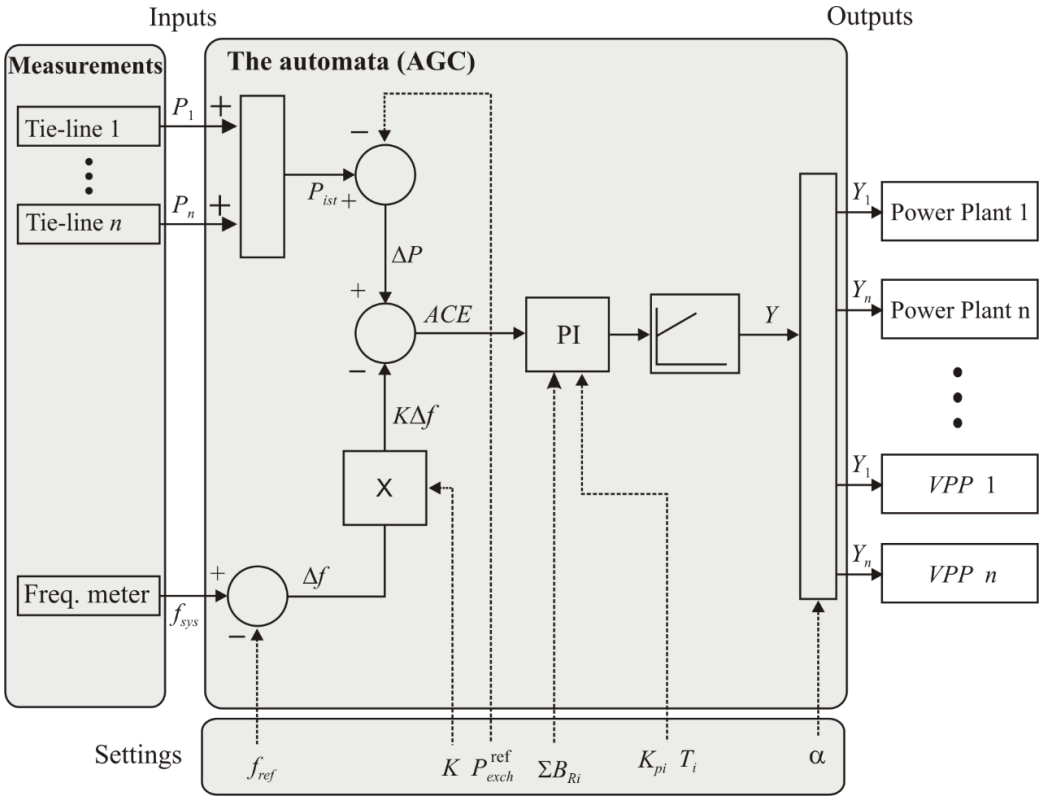

Figure B.3: AGC control scheme.

The deviation resulted from the combination between the area power unbalance and frequency deviation results in an area control error (ACE), which is passed through a PI regulator. The output of the AGC regulator consists in control signals sent to the controllers of the power plants as well as to the VPP control.

B.4 Characteristics of the Romanian Power System

A diagram of the Romanian transmission system (RTS) is shown in Figure B.4. The RTS is interconnected with the power systems of Moldova, Ukraine, Hungary, Serbia and Bulgaria.

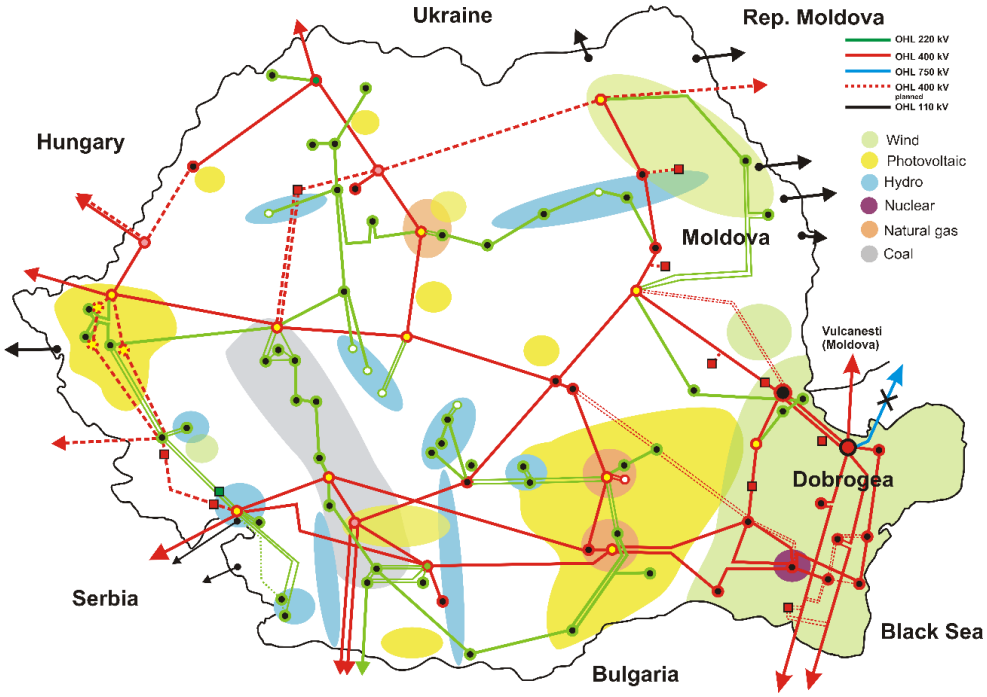

Figure B.4: Single-line diagram of the Romanian Transmission Network.

The Romanian transmission system consists of:

- 81 substations, including one 750 kV substation, 38 substations at 400 kV, and 42 substations at 220 kV, as well as approximately 216 transformers with a total installed power of 38,058 MVA;
- 8,834.4 km of transmission lines encompassing 3 km of 750 kV lines, 4912 km of 400 kV lines, 3,875.6 km of 220 kV lines, and 40.4 km of 110 kV lines, of which 486.2 km of interconnection lines.

The supervision of System operation is performed by a centralized SCADA/EMS system, which plays two major roles: (i) it is responsible for the real-time acquisition and processing of all data pertaining to the operation of the RTS, and (ii) it provides the monitoring of operation and remote control of approximately 350 generators and 660 substations under the operational jurisdiction of the National Dispatch Centre (NDC) and five Territorial Dispatch Centres. NDC (also called UnODEN in Romanian) is the administrative entity that monitors, supervises, and controls the power system. There are five Territorial Dispatch Centres located in Bucharest, Timisoara, Craiova Bacau and Cluj. The Bucharest Dispatch Centre (BDC) is located in the same building as the NDC.

Some observations can be made about the geographic location of the power plants:

- The coal-fired power plants are located in the same area, as indicated by the gray color;
- Few large gas-fired power plants, running all year, are located in two positions. During winter, city power plants are used to produce combined heat and power;
- The hydraulic power plants are spread in a large area, and the generation is shared between run-of-river and storage-dam power plants in balanced proportion;
- Out of the 3,025 MW 1wind capacity installed in Romania, about 86% (∼2,600 MW) are

in the Dobrogea region, near the Black Sea. The remaining 14% is mostly located in the North-East of the country;

- A 2x700 MW nuclear power plant is also located in Dobrogea. Thus more than 4,000 MW of installed power are concentrated in this region;
- Photovoltaic power plants are spread all over the country. However, the largest power share is located in the south of the country.

According to [51], in 2015 the demand for approval of new wind power plants was about 4,550 MW in Dobrogea only. Furthermore, there are requests for approval of new wind power plants in the Moldova region of Romania. All these projects are in stand-by, while no wind power plant was commissioned in 2017 because of the change in the legislation for supporting renewable energy sources by green certificates.

The coal- and gas-fired power plants, most of them located in South Romania, will be replaced with RES based power plants, also located in the south. The transmission network may not require dramatic changes in the configuration, however, new transmission lines may be required to relay the power produced in Dobrogea region. It is foreseen that construction of new AC transmission lines is more and more difficult because of the cost of the land, and therefore, HVDC technology will be adopted.

The simulations have been performed in Eurostag.[1] A simplified network of 195 buses has been used, which includes the 400 kV and 220 kV buses, as well as MV buses of the generation units together with the corresponding unit transformers. When necessary, lower level buses employed by the generation units have also been included. Note that the configuration of the power system used for simulations includes future developments to accommodate for more wind power generation in the Dobrogea region and also to upgrade the west side ring from 220 kV to 400 kV. A few external buses from neighbor power systems have also been included. The total load considered in Romania is 7,142 MW (area 44), and the external load is 1,117 MW (area 11). The external load is covered by export from the Romanian power system, which means that no external generator was represented. This assumption is based on the fact that at high level of power generation from wind, Romania is a net power exporter. The load flow power balance resulted from Eurostag simulation is presented below:

Table B.1: WSCC 9-bus System Machine Data.

Area	Active power (MW)			
	Generation	Load	Losses	Export
11	0.00	1117.98	2.84	-1120.82
44	8466.37	7142.32	203.23	1120.82
Total	8466.37	8260.30	206.08	-0.01
	Reactive Power (MVAr)			
	Capacitors			-398.81

In the dynamic simulations, only the hydro and nuclear units have been considered, besides the wind units.

B.5 Numerical Simulations

B.5.1 Primary Frequency Control

Case 1 – Power Unbalance

The first simulation performed on the Romanian power system database aims at evaluating the importance of BESSs in frequency stability and control. A sudden load connection of 245 MW,

[1] The Eurostag website is available at http://www.eurostag.be/

which represents 2.9% of the total generation, was assumed. Figure B.5 illustrates the frequency variation, in the case with and without storage. Although in the case without storage the frequency is stabilized, the quasi-steady state value is outside the normal range, and can trigger the tripping of some equipment. The rapid contribution of about 155 MW from the BESS helps maintain the frequency within a more acceptable deviation range. Beyond the simulation time window, the upper control levels may intervene to restore the BESS reserve.

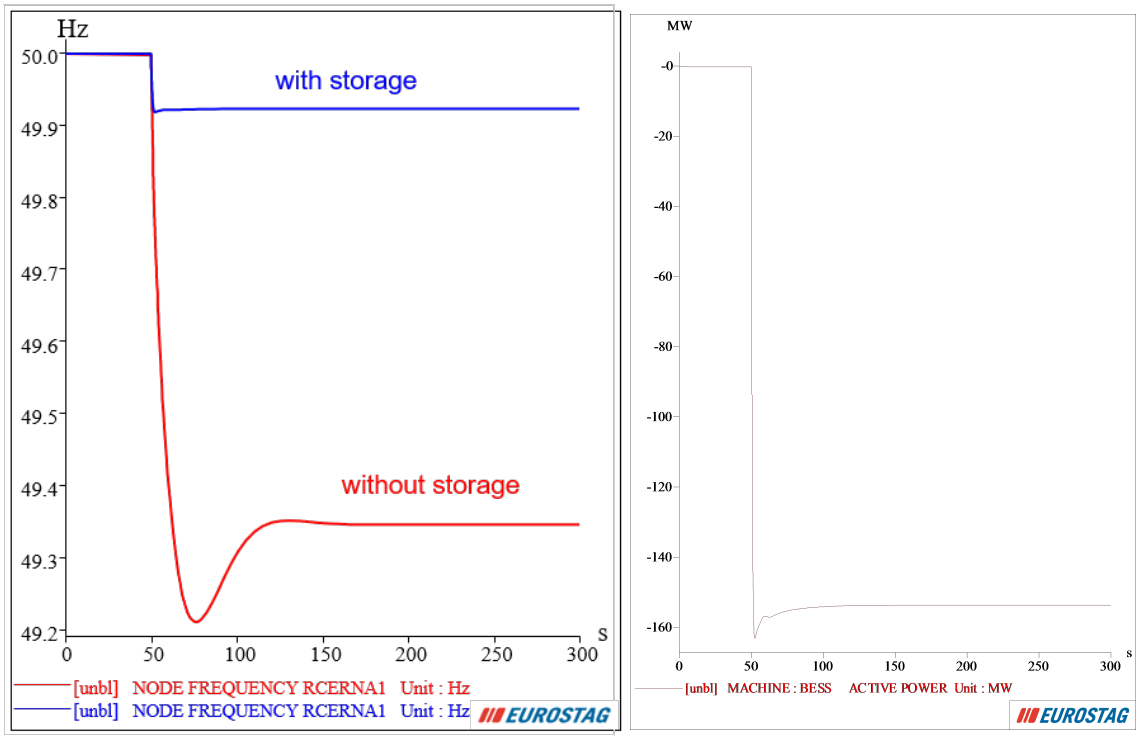

(a) Frequency variation. (b) BESS active power injection.

Figure B.5: Sudden/uncontrolled disconnection of a 245 MW load.

Either for a fast or a slow frequency containment (primary) control, the next level capable or designed to replace the BESS reserve is the secondary (AGC) level. The secondary control level is a slow action, which may delay the replacement of the BESS and involves using more storage energy than economically effective. For this reason, if the power system relies on very fast primary actions, the time response of the secondary control level should be shortened.

Case 2 – Loss of a Large Generation Unit

The largest generation units in the Romanian power system are the 700 MW rated units of the Cernavoda Nuclear Power Plant. The ancillary service of one such units accounts for about 6% of the rated power. In the simulation, we have assumed that the steady state value of 660 MW was lost, together with all associated dynamic models.

Eurostag simulation results of the Romanian power system database reveal that the system stability is quickly lost. However, in the real operation of the Continental power system of ENTSO-E, the tripped unit represents an almost insignificant contribution to the total generation. This is shown in deliverable D5.5, which illustrates the frequency variations, recorded by means of PMUs, where the influence of a similar unit is exhibited.

In order to maintain the system stability, we have considered the use of a BESS, of various rated powers. Figure B.6 shows the frequency after generator tripping, for 6 values of the rated power of the BESS. The presence of a 300 MW BESS leads to a 3 Hz frequency excursion. As the rated

power of the BESS is reduced, the frequency exhibits increasing oscillations. A 30 MW rated BESS ensures the system stability, but with amplitudes of the frequency oscillations that can trigger some protection systems or can lead to desynchronization of interconnected systems. On the other hand, a 20 MW rated BESS is not capable of maintaining the system stability; this is a case of first swing instability. Therefore, small rated BESSs can help maintaining the stability, but the frequency nadir could be unacceptably low.

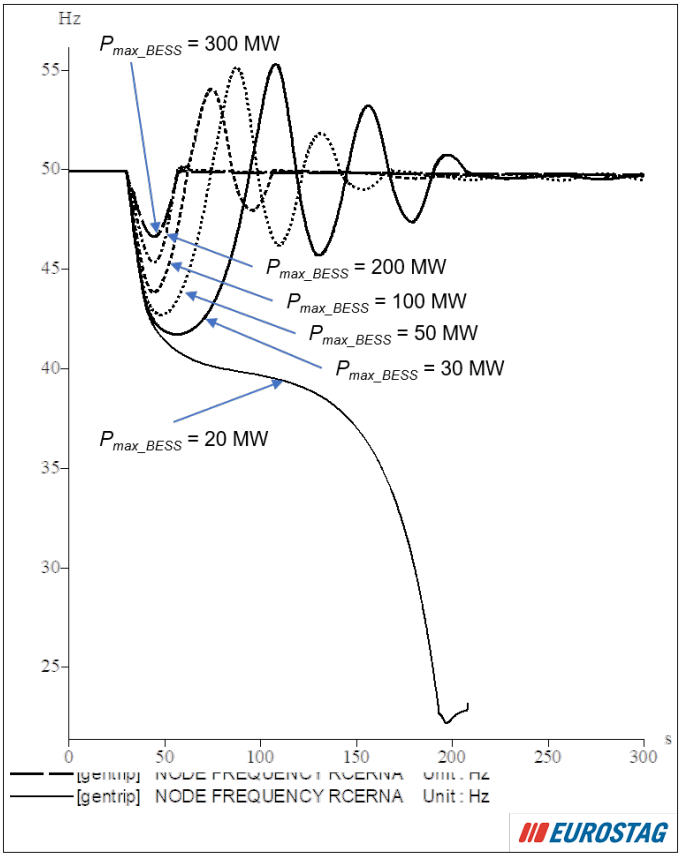

Figure B.6: Sudden/uncontrolled disconnection of one nuclear unit (660 MW).

As also shown in deliverable D2.2, the power reserve is very important for frequency stability and fast recovery. Therefore, when used for fast frequency control, the power rating of a BESS or similar system should be sufficiently large. The following moments taken to restore the frequency, within the secondary frequency control level, can require large reserves of energy available not only in electrochemical storage systems but also in large power plants designed for this purpose, such as the pumped-storage hydro units. The energy transition requires not only a change in the energy generation paradigm, but also in the power market and the organization of the monopolar network operator. This is because, for social reason, the new grid requirements could not be affordable for all countries.

B.5.2 Secondary Frequency Control

Case 3 – Power Unbalance

The secondary control actions are activated only if the frequency falls within some acceptable ranges after a disturbance. Large frequency variations require immediate manual actions by the power system operator, as force majeure action. This involves immediate activation of tertiary reserves, manual load shedding, as additional measures to the automatic load shedding. For this reason, the simulation of the secondary frequency control makes sense for cases in which frequency can reach a quasi-steady state.

We assume the same contingency as in the case of simulation of the primary frequency control actions assuming a power imbalance of 245 MW caused by the connection of load. This is similar to the disconnection of a generation unit leading to the same power unbalance.

Figure B.6 shows the power contribution of the Lotru Hydro Power Plant and the BESS to recover (FCC) and restore (aFRC = AGC) the frequency after the occurrence of the 245 MW power unbalance. Therefore, in this simulation both the FCC and aFRC control are active. Note that Lotru Hydro Power Plant (HPP) is the most effective power plant in Romania to provide fast control in aFRC. Also, by convention in Eurostag, the generation of an injector type machine, as it is the case of BESS, the power injection is represented by negative sign.

Similar to Case 1 above, the BESS is faster than the hydro units and acts almost instantly to limit the frequency nadir and recover the frequency. The frequency containment reserve of the BESS is then gradually replaced by the automatic frequency restoration reserve. This is seen in Figure B.7.c where block 5 exhibits the control signal of the FCC loop, and block 12 exhibits the control signal of the aFRC loop – received from the central AGC, both expressed in per unit. The BESS contribution is stabilized around 40 MW as a consequence of the massive contribution from the hydro units. Note that the power contribution in aFRC is determined in Eurostag proportional to their maximum power capacity, that is 100 MW for BESS and 170 MW for the hydro units. Figure B.8 illustrates the frequency variation in the case with and without contribution from BESS. However, the Lotru hydro units are active in both cases.

The BESS importance is obvious. As shown earlier, the frequency nadir is much higher than in the case without BESS. The hydro units are not fast enough to limit the frequency drop and therefore, in the case with very low mechanical inertia they could not save the system from fast frequency instability (see Figure B.6). However, with the contribution of the BESS in the first moments, the hydro units can satisfactorily take the responsibility of restoring the frequency, eventually in almost similar time no matter of the presence of the BESS.

B.5.3 Virtual Power Plants

The aim of the simulation of a VPP is to show the importance of the storage systems and the aggregated control in reducing the power unbalances and the frequency variations.

Let us consider a VPP consisting of three entities, i.e. the wind power plant Tariverde3, the hydro unit Lotru1, and a BESS located at the 400 kV bus of Tariverde3 wind power plant.

In steady state Tariverde3 produces 11 MW out of the 117 MW as installed power. The dynamic model implemented in Eurostag calculates the corresponding initial wind speed, which is 5.32 m/s. The BESS initial power is 0 MW, and the steady state power of Lotru1 is 30 MW.

The simulation assumes 15 step changes in the wind speed, every 10 seconds by 0.1 m/s. Therefore, the wind speed achieves a steady value of 8.82 m/s at the instant 150 seconds from the simulation starting. This change in the wind speed results in a change in the active power generation from 11 MW to 26.47 MW, which means an increase of 15.47 MW in the active power generation.

The uncontrolled change in the power generation from the wind power plant is balanced by both the BESS and the hydro unit. Since the wind plant increases the power, the hydro unit reduces its generation, while BESS is charging (negative power) (Figure B.9). As the powers are balanced, the frequency is restored to the nominal value within a few minutes after the power unbalance.

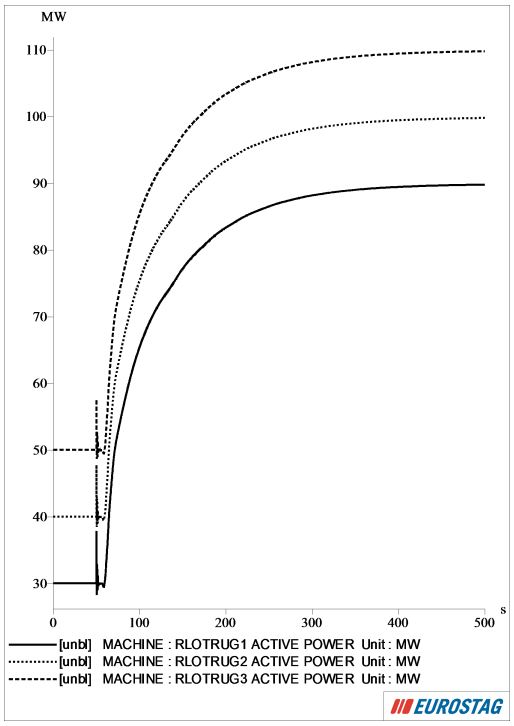

(a) Lotru HPP total response.

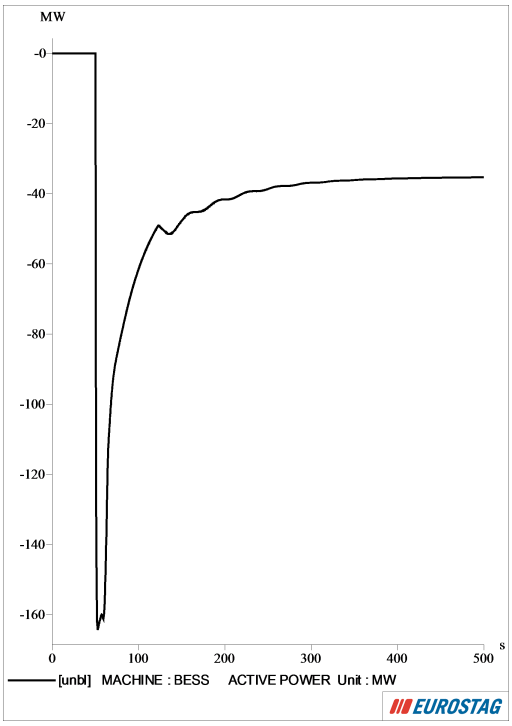

(b) BESS overall response.

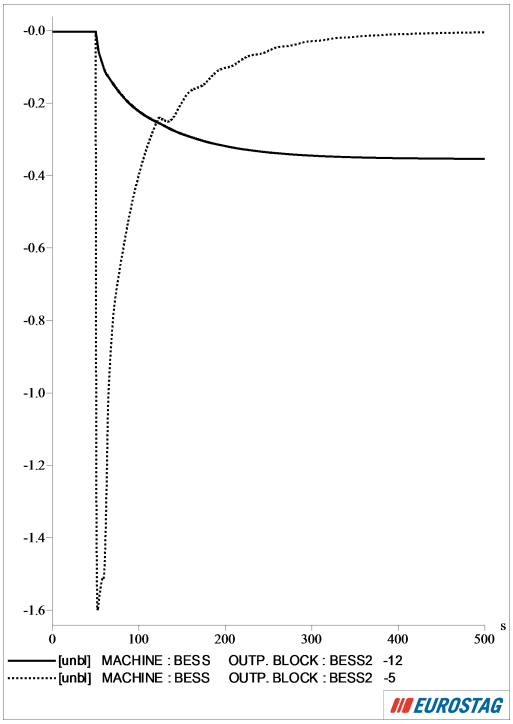

(c) BESS individual orders in per unit (solid line: AGC order, dotted line: FCC order)

Figure B.7: Power generation as AGC and FCC response in case of a 245 MW unbalance.

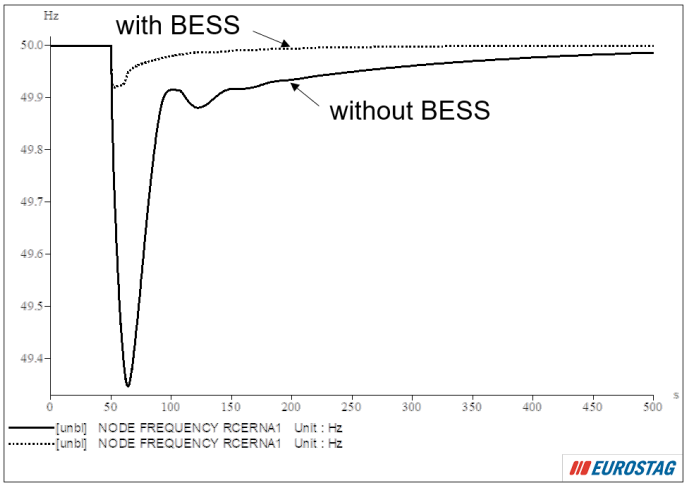

Figure B.8: Frequency variation in case of a 245 MW unbalance, with and without BESS.

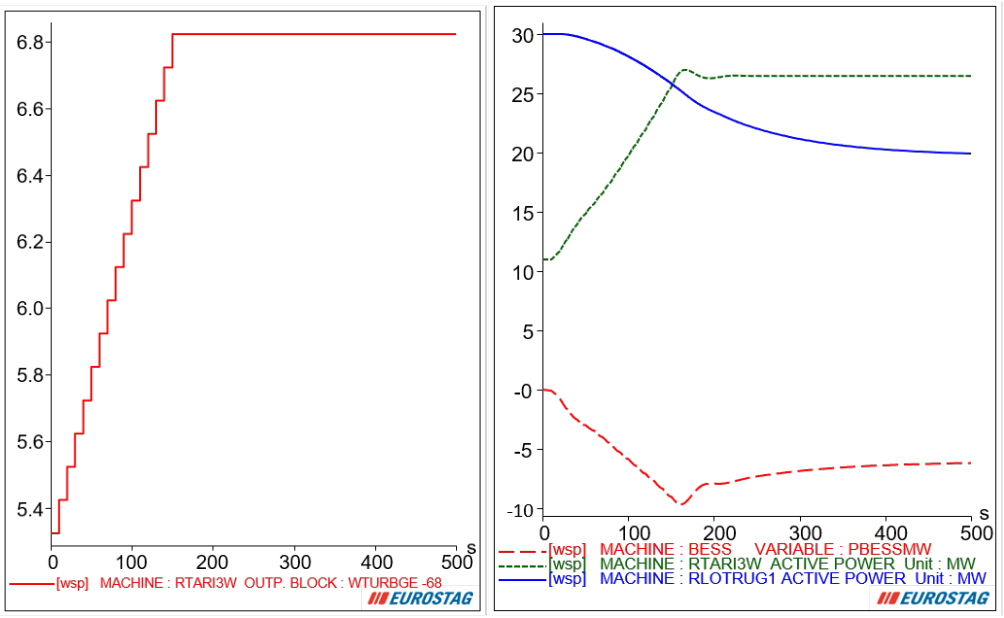

(a) Step change in the wind speed. (b) Active power generations.

Figure B.9: VPP operation.

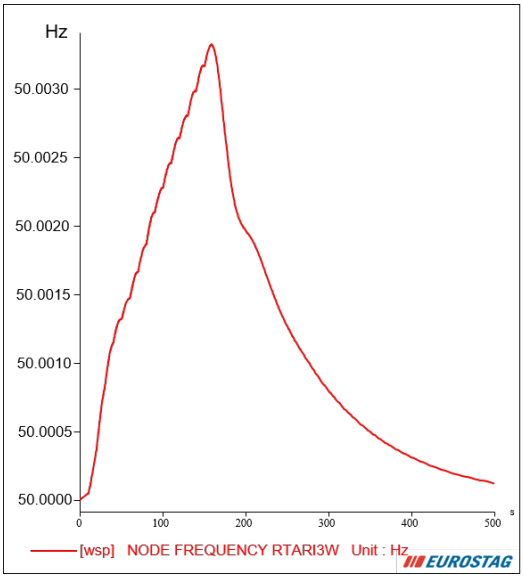

Figure B.10: Frequency variation caused by uncontrolled change in the generated power from wind.

C. Provision of Inverter-based Frequency Control in 100% Non-synchronous Systems

C.1 Frequency Control of RES-tied Converters in Zero Inertia Power Grids

C.1.1 Case Study Description

The case study of the inverter-based frequency control in 100% non-synchronous systems is based on the WSCC 9-bus 3-machine test system as shown in Figure C.1.

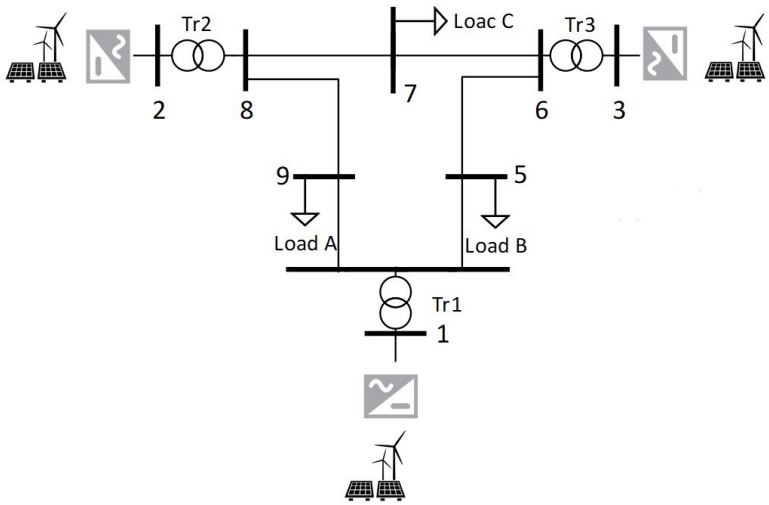

Figure C.1: Inverter-based WSCC 9-bus System

The total load is 315 MW. The test system contains 6 transmission lines, three loads and three inverter-interfaced generation connected to the network through step-up transformers at 230 kV transmission level voltage. The system parameters are given in Table C.1.

Table C.1: WSCC 9-bus System Machine Data.

Parameter	Generator #		
	1	2	3
Rated Power (MVA)	247.5	192	128
Rated Voltage (kV)	16.5	18	13.8
Inertia Constant H (s)	5	6.4	3.01

C.1.2 Decentralized LSD in Multi-machine System

In this Section, we extend the LSD concept proposed for a Single-Machine Infinite-Bus (SMIB), to achieve a decentralized LSD control in a multi-machine system. As presented in deliverable D2.3, the LSD concept i.e. the linearization of the per-unit nonlinear swing equation (C.1) emulated in the VSG has been achieved through voltage control, considering that voltage has to be maintained within certain limits. In equation (C.1), δ is the angle between the voltage at the infinite bus, E, and the converter output voltage, V; $\omega = \dot{\delta}$ is the angular speed; P_m is the converter power set-point; M and D are the emulated inertia and damping of the VSG, respectively; and X is the network impedance.

$$M\dot{\omega}(t) = P_m(t) - \frac{E\,V(t)}{X}\sin\delta(t) - D\,\omega(t)\,. \tag{C.1}$$

For the SMIB system shown in Figure C.2, X and E are constants. In the proposed solution (see Deliverable D2.3) the voltage can be controlled within certain limits of the nominal voltage value, E_{nom}. For the SMIB, the infinite bus voltage E is equal to E_{nom} , hence the control law is derived as follows:

$$P(t) = \frac{E_{\mathrm{nom}}\, V(t)}{X} \sin\delta(t) = \frac{E_{\mathrm{nom}}}{X}(1-\varepsilon)\, E_{\mathrm{nom}}\, \delta\ , \tag{C.2}$$

where ε determines the slope of the linearized characteristic, and it needs to be chosen in order to ensure that the output voltage remains within the allowed limits.

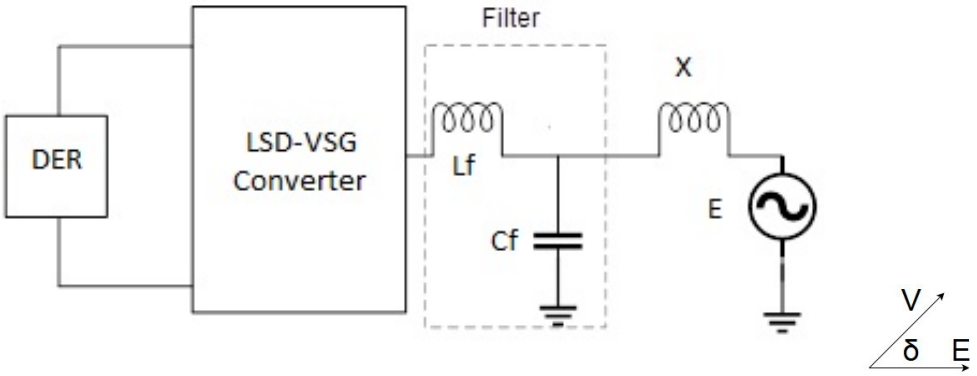

Figure C.2: Single-Machine Infinite-Bus system.

The reference angle δ and the reference voltage V are calculated as:

$$\delta(t,P) = \frac{P(t)\, X}{(1-\varepsilon)\, E_{\mathrm{nom}}^2}\ , \tag{C.3}$$

$$V(t,\delta_{\mathrm{r}}) = \frac{(1-\varepsilon)\, E_{\mathrm{nom}}}{\sin\delta(t)}\, \delta(t)\ . \tag{C.4}$$

The linearized system can thus be written as follows:

$$\begin{bmatrix} \Delta\dot{\delta}(t) \\ \Delta\dot{\omega}(t) \end{bmatrix} = \begin{bmatrix} 0 & 1 \\ -\dfrac{(1-\varepsilon)\, E_{\mathrm{nom}}^2}{M\, X} & -\dfrac{D}{M} \end{bmatrix} \begin{bmatrix} \Delta\delta(t) \\ \Delta\omega(t) \end{bmatrix}\ . \tag{C.5}$$

Similarly, this approach can be extended to a multi-machine system, by representing the rest of the system seen by each machine by the Thevenin equivalent circuit i.e. a voltage source behind a constant impedance.

In a multi-machine machine power network, the generators and loads are located at different nodes, hence, the model can be expressed in terms of differential algebraic equations (DAEs), where the algebraic constraints represent the load characteristics. In order to represent the system in terms of ordinary differential equations (ODEs), the derivation of a network reduced model is needed. The Kron Reduction [27] is a popular model reduction method. In this method, the algebraic constraints variables (e.g. loads) are solved in terms of the rest of the variables. A drawback of the Kron Reduction is that it is limited to constant admittance loads. In the case of constant power loads (CPLs), the algebraic constraints are proper, hence they are not explicitly solvable. For the network reduction with CPLs, the approach proposed in [35] is used. It is worth mentioning that the obtained admittance matrix does not correspond to any physical wires or lines but just fictional ones because of network reduction.

Hence, the 9-bus system shown in Figure C.1 becomes a 3-bus system consisting of three trans-

mission lines, with all the nodes that do not have generators directly connected to them eliminated.

After achieving the reduced model with only generator nodes, the Thevenin impedance seen by each machine can be calculated from the obtained admittance matrix $\bar{\boldsymbol{Y}}_{\mathrm{bus}}$, by first calculating the $\bar{\boldsymbol{Z}}_{\mathrm{bus}}$ matrix:

$$\bar{\boldsymbol{Z}}_{\mathrm{bus}} = \bar{\boldsymbol{Y}}_{\mathrm{bus}}^{-1} = \begin{bmatrix} \bar{Z}_{11} & \dots & \bar{Z}_{1n} \\ \vdots & \ddots & \vdots \\ \bar{Z}_{n1} & \dots & \bar{Z}_{nn} \end{bmatrix} . \tag{C.6}$$

The Thevenin impedance at bus i is thus:

$$\bar{Z}_{\mathrm{th},i} = \bar{Z}_{ii} . \tag{C.7}$$

It is worth noting that with CPLs, the Thevenin impedance will not depend on the load value but only on the topology. Hence, for a given topology, the Thevenin impedance is constant.

As for the Thevenin voltage seen by each machine at its terminals, the Root-Mean-Squared value can be calculated from the local active and reactive power measurements. In an inductive network the active power and reactive power are given as follows:

$$P_i(t) = \frac{E_{\mathrm{th},i}(t)\, V_i(t)}{X_{\mathrm{th},i}} \sin \delta_i(t) , \tag{C.8}$$

$$Q_i(t) = \frac{E_{\mathrm{th},i}(t)\, V_i(t)}{X_{\mathrm{th},i}} \cos \delta_i(t) - \frac{V_i^2(t)}{X_{\mathrm{th},i}} . \tag{C.9}$$

Combining (C.8) and (C.9), the reactive power is given as follows:

$$Q_i(t) = \sqrt{\left[\frac{E_{\mathrm{th},i}(t)\, V_i(t)}{X_{\mathrm{th},i}}\right]^2 - P_i^2(t)} - \frac{V_i^2(t)}{X_{\mathrm{th},i}} . \tag{C.10}$$

Consequently, $E_{\mathrm{th},i}$ can be calculated as:

$$E_{\mathrm{th},i}(t) = \frac{X_{\mathrm{th},i}}{V_i(t)} \sqrt{\left[Q_i(t) + \frac{V_i^2(t)}{X_{\mathrm{th},i}}\right]^2 + P_i^2(t)} . \tag{C.11}$$

The output voltage of each machine is controlled as follows:

$$V_i(t, \delta) = \frac{(1 - \varepsilon_i)\, E_{\mathrm{nom}}}{\sin \delta_i(t)}\, \delta_i(t) . \tag{C.12}$$

Finally, the dynamic model for machine i can be expressed as follows:

$$\begin{bmatrix} \Delta\dot{\delta}_i(t) \\ \Delta\dot{\omega}_i(t) \end{bmatrix} = \begin{bmatrix} 0 & 1 \\ -\dfrac{(1 - \varepsilon_i)\, E_{\mathrm{nom}}\, E_{\mathrm{th},i}(t)}{M_i\, X_{\mathrm{th},i}} & -\dfrac{D_i}{M_i} \end{bmatrix} \begin{bmatrix} \Delta\delta_i(t) \\ \Delta\omega_i(t) \end{bmatrix} . \tag{C.13}$$

Unlike the SMIB case, the Thevenin voltage is not constant, thus the system matrix of (C.13) it is not constant either. In order to achieve linear and uniform dynamics, the system matrix should remain constant. Consequently, it is not enough to just control the voltage.

Unlike synchronous machines where inertia and damping are determined by the physical design, the power converters controlled as virtual synchronous machines face no such constraints. Hence, the emulated inertia M and damping D can be adaptively adjusted online to keep the system matrix constant when E_{th} changes or even when the topology i.e. X_{th} changes, as formulated below:

$$M = M_{\text{nom}} \frac{E_{\text{th}}(t)}{E_{\text{nom}}}, \tag{C.14}$$

$$D = D_{\text{nom}} \frac{E_{\text{th}}(t)}{E_{\text{nom}}}, \tag{C.15}$$

where M_{nom} and D_{nom} are the nominal values of the emulated inertia and damping, respectively.

C.1.3 Simulation Results

Different tests cases are conducted to further validate the proposed solutions for frequency control in inverter-based 100% non-synchronous systems. The test cases cover large disturbances in the system represented by a load step of 90 MW at Bus 5 at $t = 10$ s and topology change represented with line 5-6 disconnection. This section includes some of the relevant results obtained.

C.1.3.1 Distributed Secondary Control

For simplicity the DAI communication network is mapped to the reduced power network obtained from Kron reduction as explained in Appendix C.1.2. The performance of the DAI secondary frequency control in transmission systems under the impact of time delays and measurement noise has been investigated. For time delays, the minimum time delay is calculated based on communication latency in fiber optics of 0.5 µs/km. Hence, for 100 km long transmission line, the minimum communication latency in the communication link, ignoring any other latencies, is 0.5 ms.

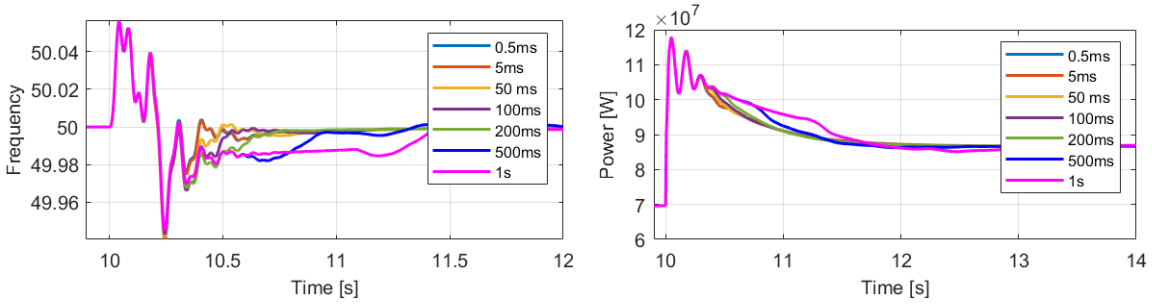

(a) Frequency response. (b) Active power injection.

Figure C.3: Response at Bus 1 following a 90 MW load step at 10 s for different time-delays in DAI control.

As depicted in Figure C.3, the DAI control manages to restore the frequency to nominal value in the presence of delays. However, for delays larger than 200 ms oscillations in the frequency can be observed. These oscillations could destabilize the system. As for the noise impact on the DAI control performance, additive noise with different variance values is applied to the DAI control outputs of neighboring converters which are to be used at the local converter to adjust its power reference in per unit. The additive noise represents environmental noise which could be modeled as Gaussian noise.

Figure C.4 shows the effect noise on the DAI control performance. From the observation of this figure, it is clear that the DAI control is noise resilient, and the controllers have desirable performance even when the noise variance is increased.

Figures C.5.a and C.5.b illustrate the frequency response at different machine buses, following a load step of 90 MW at 10 s, without and with DAI control, respectively. The results indicate clearly that the control hierarchy between the secondary and primary control disappears with the DAI control. It can be observed that the DAI control interaction with the primary control minimizes the frequency nadir at Bus 3 and 2. Moreover, it can be observed from Figure C.5 that with 100% non-synchronous grid, the response of the system is so fast that the frequency across different buses differs so much during transients. It is also worth mentioning that the depicted frequency response represents the PLL measurements. However, in the VSG control structure, the PLL frequency is used only in implementing the damping term of the swing equation, while the internally generated VSG frequency, based on the power-balance, is used in the primary droop control and internal control loops [6]. Figure C.6 shows that the VSG frequency is less volatile compared with PLL measured frequency at the same bus.

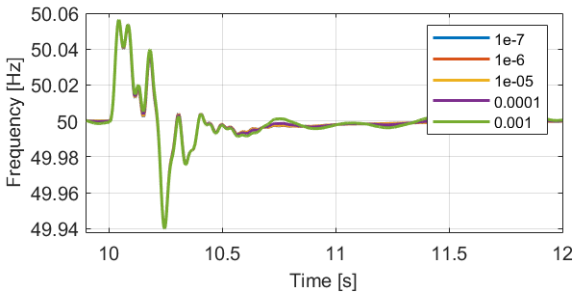

Figure C.4: Frequency response at Bus 1 following a load step for different measurement noise variance.

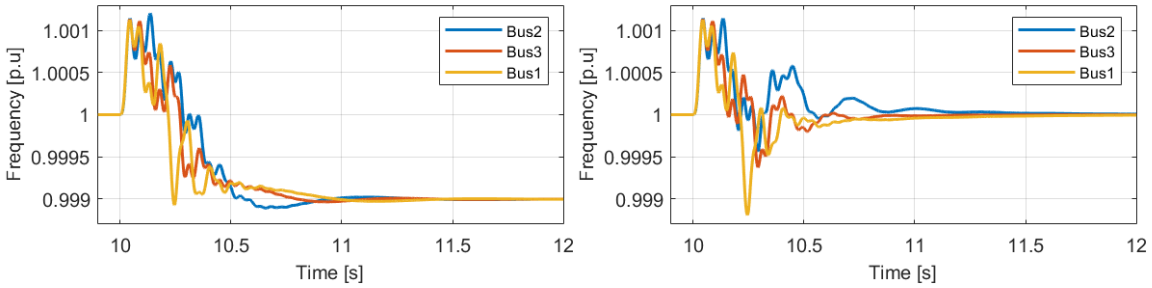

(a) Without DAI control. (b) With DAI control.

Figure C.5: Frequency at different buses.

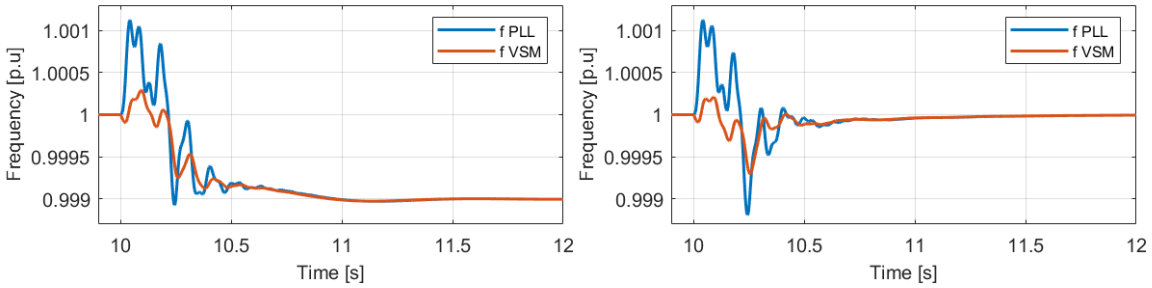

(a) Without DAI control. (b) With DAI control.

Figure C.6: Comparison between PLL frequency and the VSG frequency.

C.1.3.2 Linear Swing Dynamics for Converter Based Power Grids

In this section we present a comparison study of the VSG and the LSD-VSG. Some relevant results are shown in the figures below.

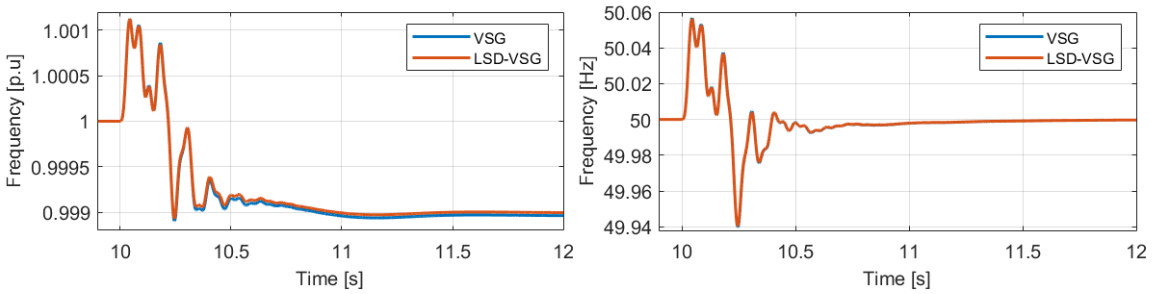

(a) Without DAI control. (b) With DAI control.

Figure C.7: Comparison of the VSG and LSD-VSG frequency response at Bus 1 following a load step.

Figures C.7.a and C.7.b compare the frequency response of LSD-VSG and VSG following a load step at 10 s without and with DAI control, respectively. It can be observed that the LSD-VSG results in smaller frequency variations. From Figure C.7.a, it is also clear that steady state frequency deviation in case of LSD-VSG is smaller compared to the VSG.

The performance of the VSG and LSD-VSG following a topology change represented with a transmission line tripping is illustrated in Figure C.8. It can be observed that although the LSD-VSG control uses the equivalent network impedance in the control law as explained in Appendix C.1.2, a change in the topology i.e. in the equivalent network impedance does not jeopardize the LSD-VSG stability.

The effect of the droop setting and the damping of virtual inertia control loop of the VSG has been also studied. For these study cases, the secondary control is not considered, to focus on the crucial effects on the frequency stability. Additionally, the droop and the damping values are set the same for all machines.

Figure C.9 shows the effect of different damping values on the frequency response. It can be seen that for smaller damping values, the frequency response is faster to reach steady state but on the other hand, smaller values result in higher frequency nadir and undesired low frequency oscillations in the range of 5-10 Hz. Larger damping values (i.e. 4 and 10 pu) result in a slower but more damped response. However, very large damping values (40 and 100 pu) could destabilize

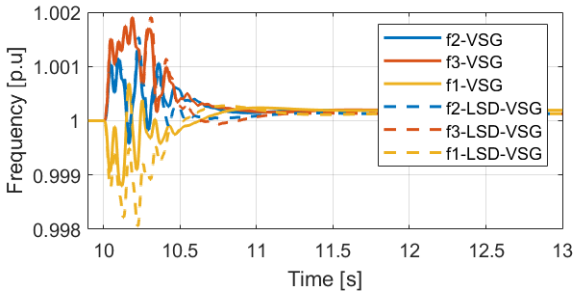

Figure C.8: Comparison of the VSG and LSD-VSG frequency response following a transmission line disconnection.

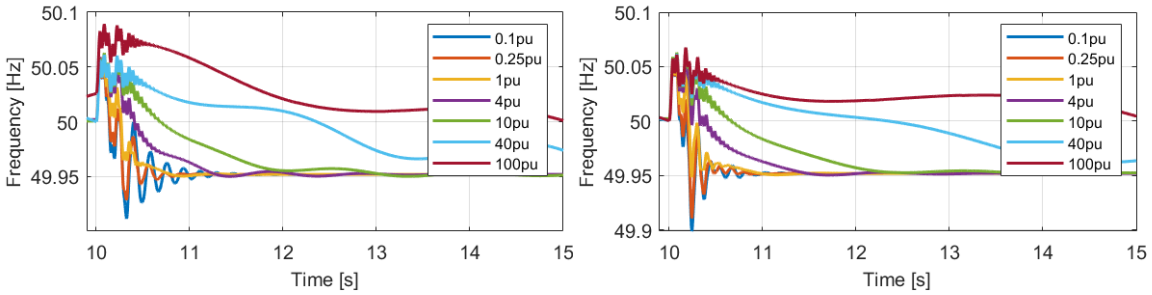

(a) Bus 1. (b) Bus 3.

Figure C.9: Frequency response following a load step for different damping values.

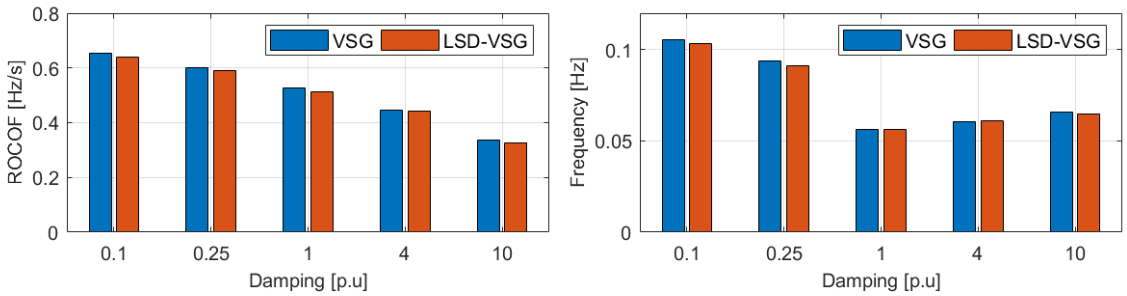

(a) RoCoF. (b) Frequency nadir.

Figure C.10: Response at Bus 1 following a load step for different damping values.

the system. Based on these results, for the given study case, a damping value of 1 pu shows an optimal performance in regards to speed and oscillations. The impact of the damping parameter on the frequency performance metrics i.e. RoCoF and frequency nadir is shown in Figures C.10.a and C.10.b, respectively. Figure C.10.a suggests that the damping value is directly linked to the RoCoF, as higher damping results in smaller RoCoF. However, as seen in Figure C.10.b, the damping affects the frequency nadir, but the relationship is not so direct. As can be observed in Figure C.9, larger damping could result in smaller frequency undershoot but higher overshoot and so the maximum frequency deviation could still be larger.

Similarly to the damping effect, the droop effect on the frequency response at Bus 1 is depicted in Figure C.11.a. Droop values between 2% and 15% are considered. However, it is worth mentioning though that according to [15], the droop settings should be between 2% and 12%. As shown, higher droop values result in higher frequency nadirs and steady sate deviations. Figure C.11.b shows that

higher droop values result in power oscillations.

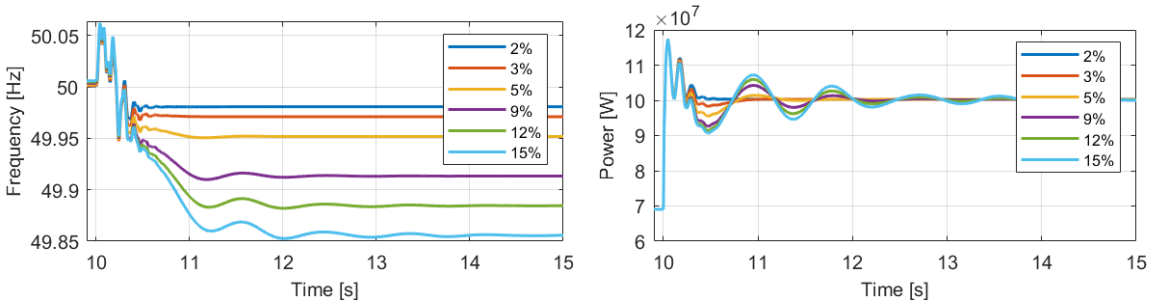

(a) Frequency. (b) Active power injection.

Figure C.11: Response at Bus 1 following a load step for different droop settings.

The impact of droop setting on the frequency performance metrics is shown in Figure C.12. Higher droop setting results in higher frequency nadir and RoCoF.

The RoCoF calculation window for the results obtained in Figure C.10 and Figure C.12 is 180 ms. This calculation window is chosen due to the converters fast dynamics. Figure C.13 illustrates the RoCoF values, following a load step, obtained for different calculation windows.

As a final remark, Figures C.10 and C.12 clearly show that LSD-VSG results in better frequency response i.e. smaller RoCoF and smaller frequency nadir.

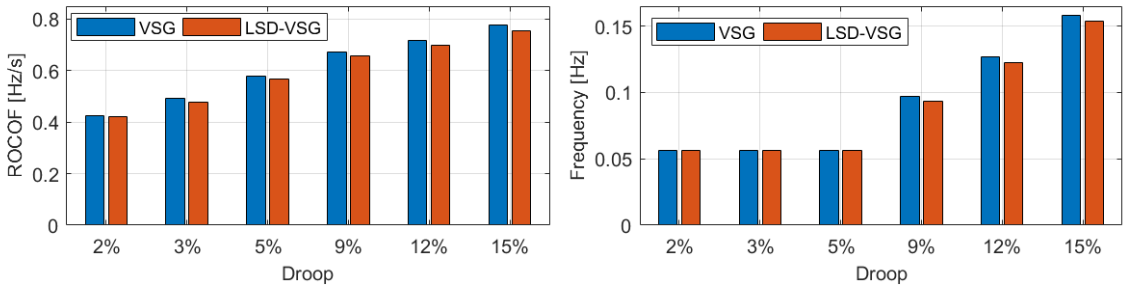

(a) RoCoF. (b) Frequency nadir.

Figure C.12: Response at Bus 1 following a load step for different droop settings.

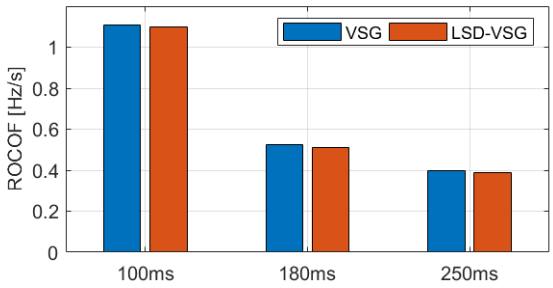

Figure C.13: RoCoF for different calculation windows.

C.2 New roles and operational characteristics of HVDC systems

C.2.1 MA-IFC scheme

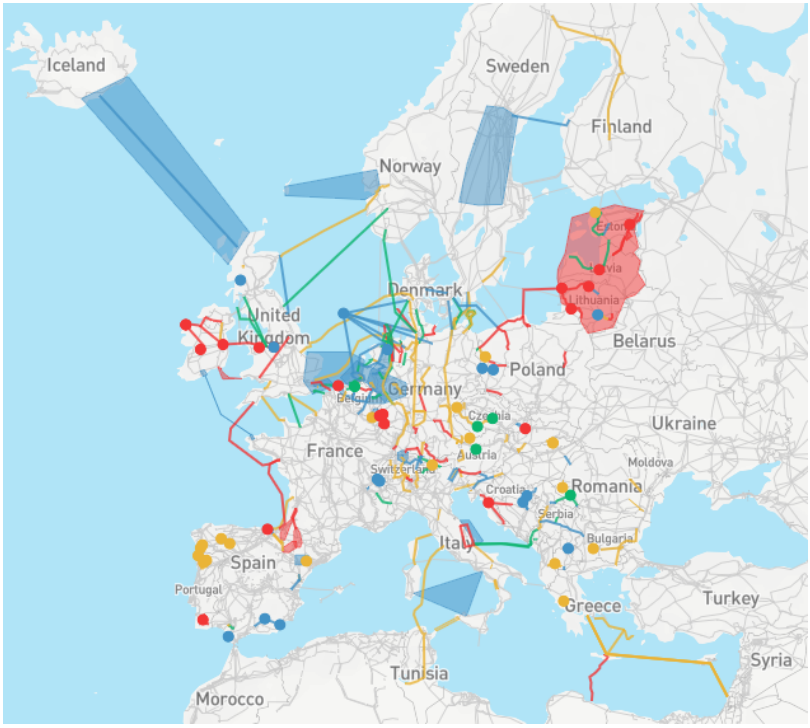

Figure C.14: ENTSO-E Ten Years Network Development Plan for 2030. Source: https://tyndp.entsoe.eu/tyndp2018/projects/

Different test scenarios are performed, and the results below show that the MA-IFC scheme provides a systematic enhancement in frequency stability, particularly in the disturbed and weak AC grids, alongside maintaining a stable DC voltage profile. Note that there is no observable deviation in DC voltage profile in case of varying $\mathcal{R}$ (in all test scenarios). Hence, the DC voltage waveform is shown once in Figure C.15.

The same test scenario (generation loss in AC1) is repeated with introducing communication delay. From the results shown in Figure C.18, the MA-IFC provide a good performance in frequency stabilization even with communication delay up to 150 ms.

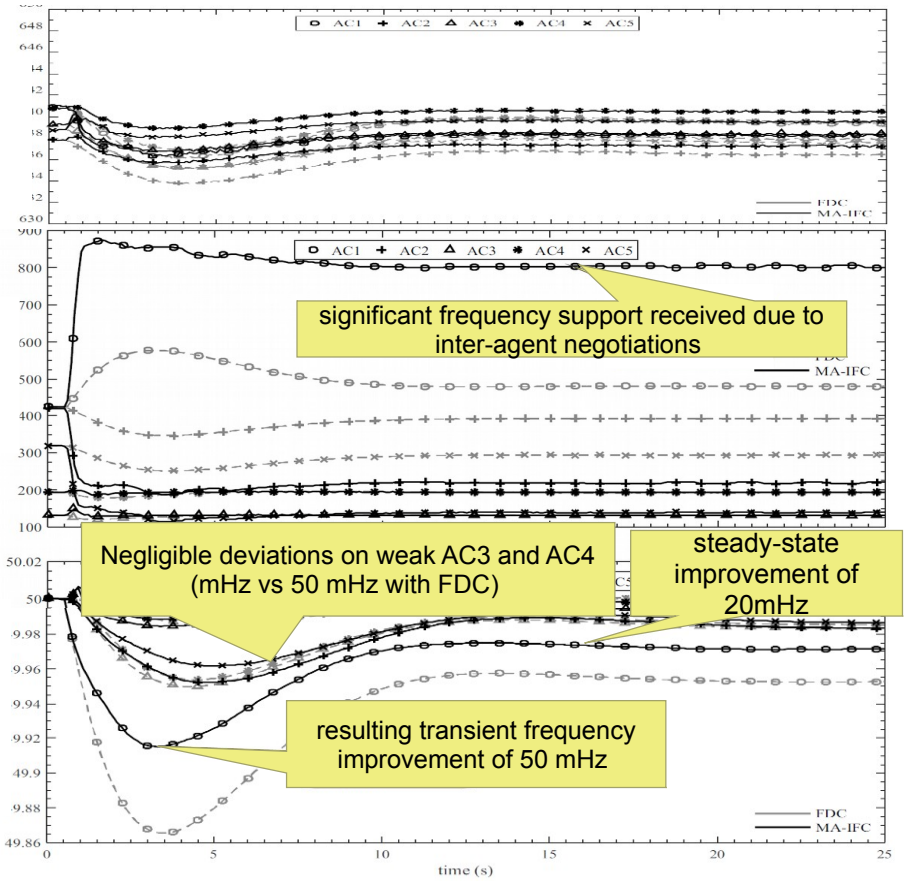

Figure C.15: Loss of generation in AC1 (comparison between MA-IFC and FDC).

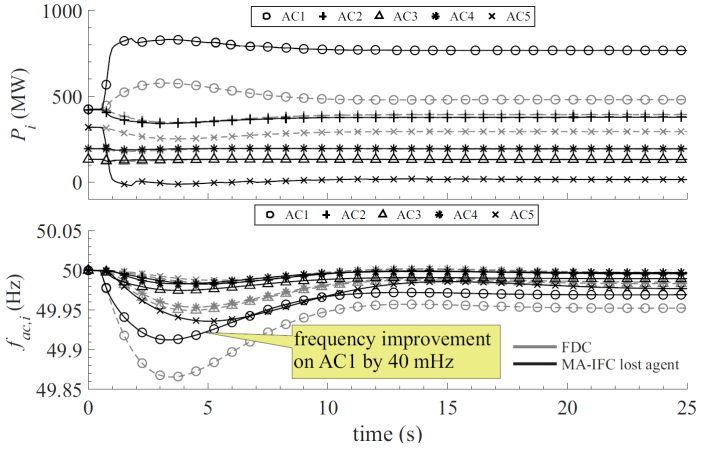

Figure C.16: Comparison between MA-IFC with agent failure and FDC.

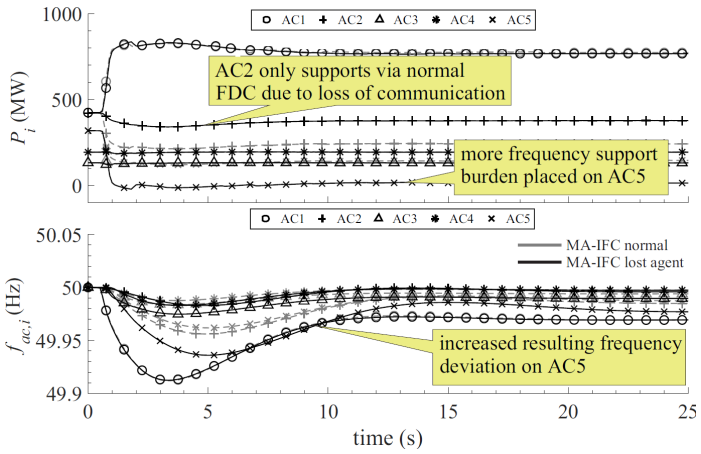

Figure C.17: Comparison between MA-IFC in normal operation and in case of agent failure.

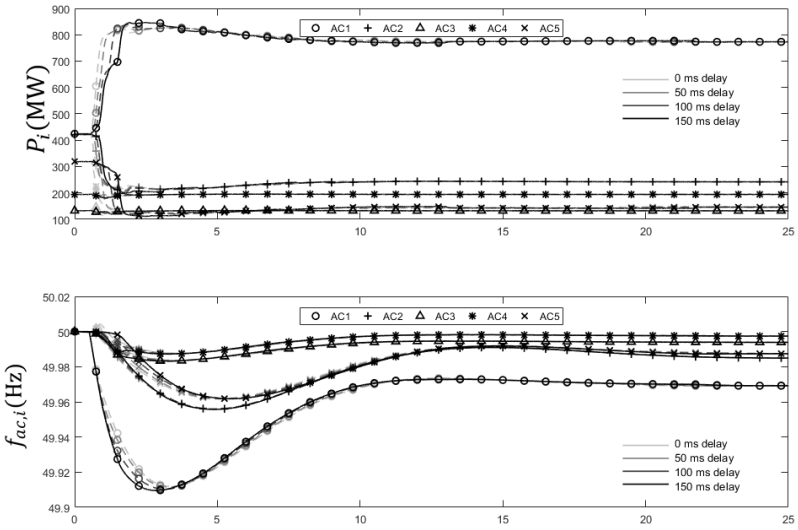

(a) Active power and frequency profile of AC grids.

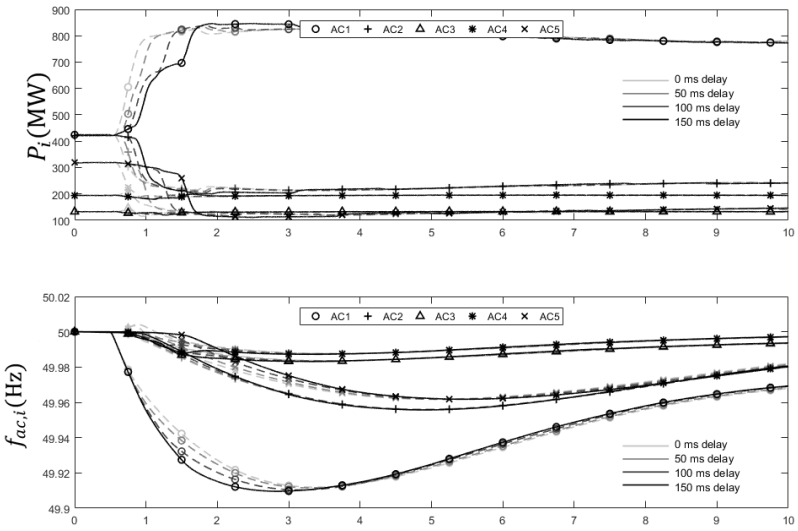

(b) Zoomed-in active power and frequency profile.

Figure C.18: MA-IFC performance under communication delay.

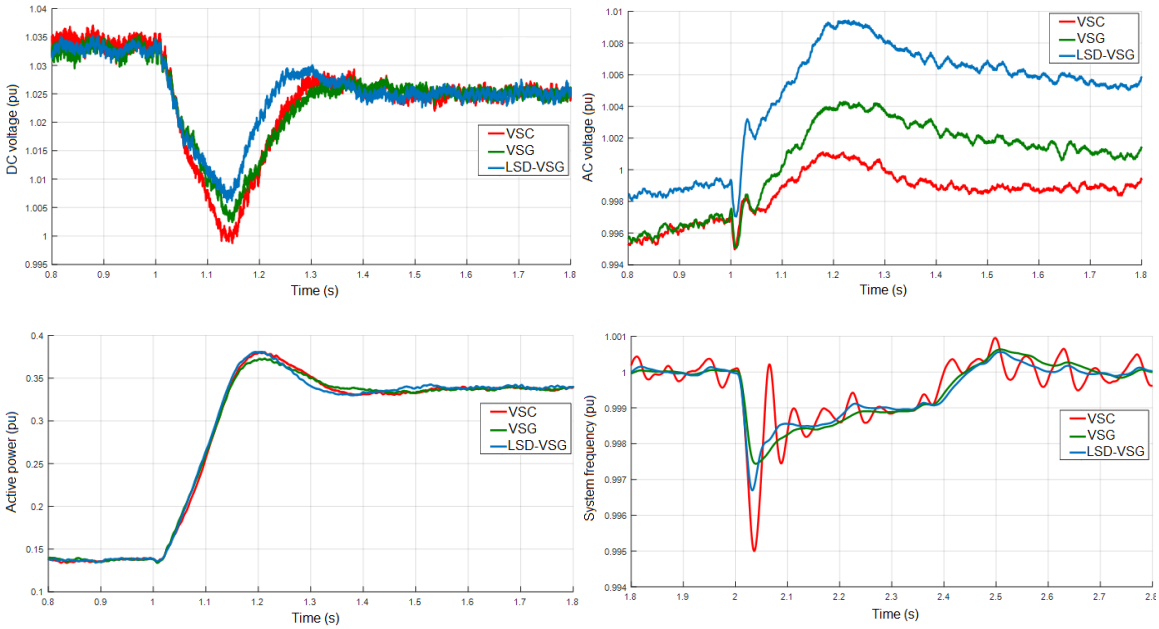

Figure C.19: Large step increase in active power demand comparison among classical VSC, VSG and LSD-VSG.

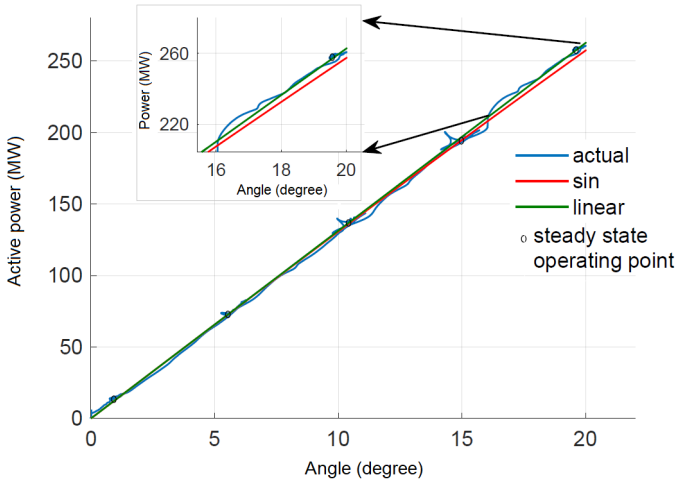

Figure C.20: Power-angle characteristics. Blue: LSD-VSG, Red: classical SG and VSG.